Phase Behavior in Iron/Carbon System

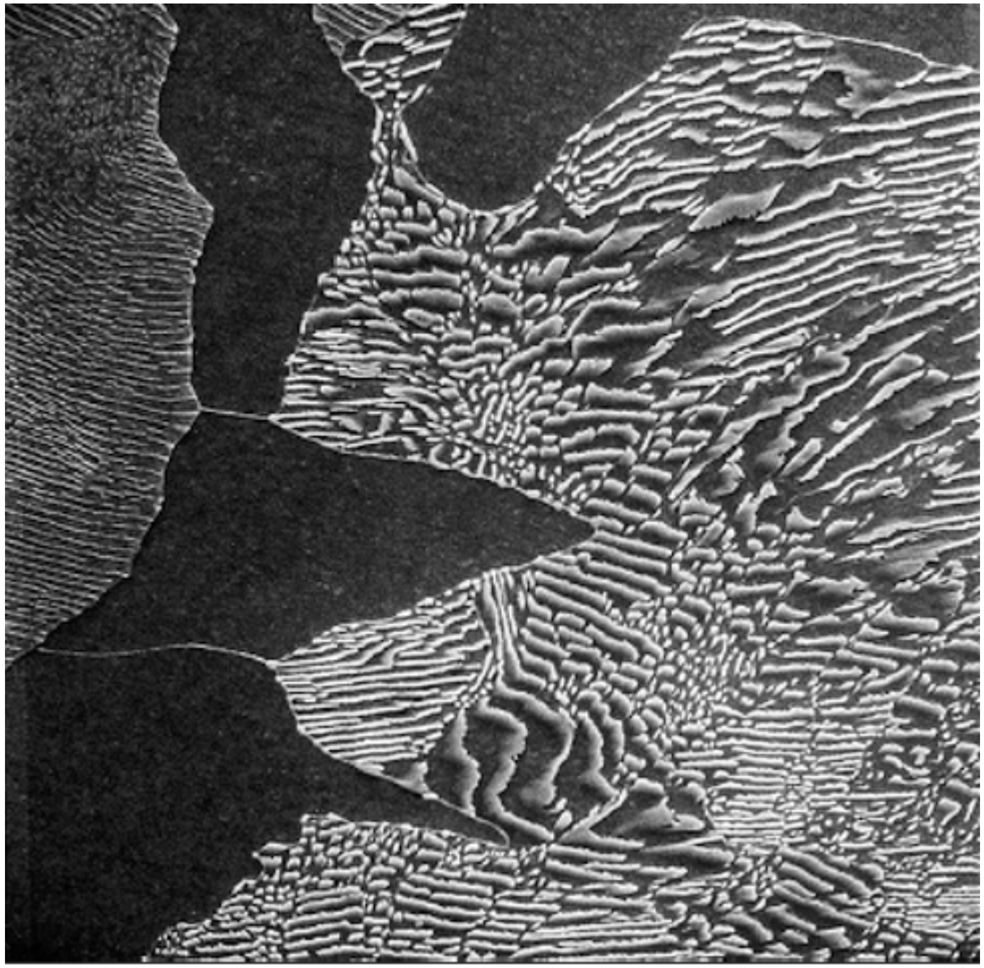

Callister P. 252
Chapter 9

A scanning electron micrograph showing the microstructure of a plain carbon steel that contains 0.44 wt% C. The large dark areas are proeutectoid ferrite. Regions having the alternating light and dark lamellar structure are pearlite; the dark and light layers in the pearlite correspond, respectively, to ferrite and cementite phases. During etching of the surface prior to examination, the ferrite phase was preferentially dissolved; thus, the pearlite appears in topographical relief with cementite layers being elevated above the ferrite layers. 3000×. (Micrograph courtesy of Republic Steel Corporation.)

Iron Age
1500 to 1000 BC

Iron Ore is extremely common and was used as a fluxing agent in copper smelting from malachite (Copper carbonate) Making an iron rich slag.

FIGURE 7.4. Major iron (and coal) deposits on the earth. (Redrawn from the *World Book Encyclopedia*, © 1997 World Book, Inc. By permission of publisher.)

Melting point is 1538°C

Iron Ore was used as a fluxing agent in copper smelting from malachite (Copper carbonate)
Making an iron rich porous slag, sponge iron.

Copper Slag contains some reduced iron as sponge iron.
Hammering compacts the sponge producing wrought iron.

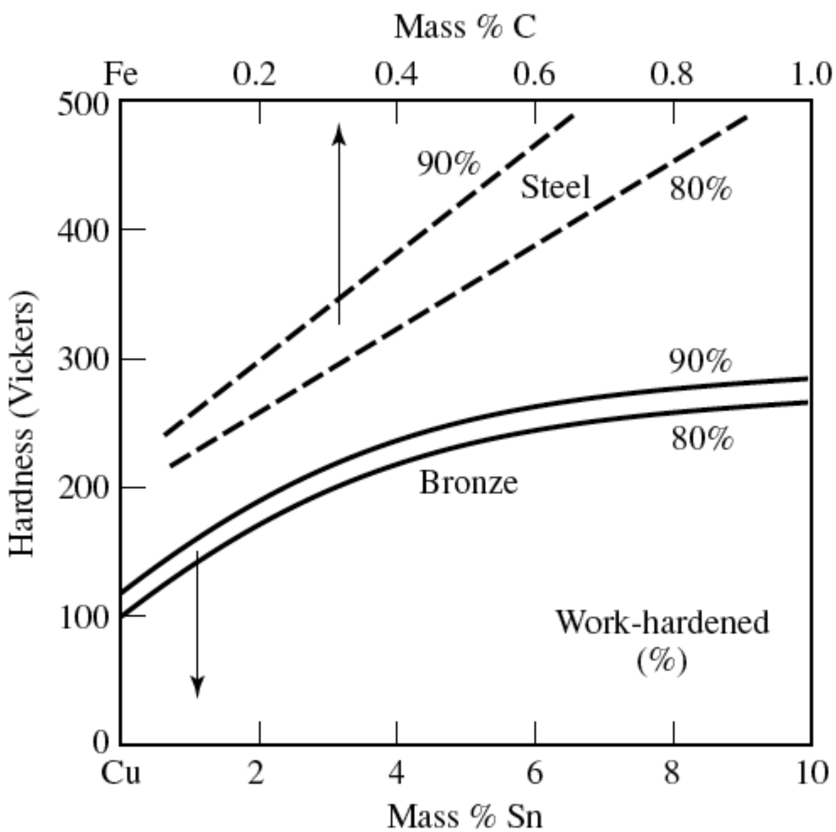

Bronze is harder than pure iron

Iron is also subject to corrosion

So pure iron is not an advancement over Bronze

Hittites (Turkey) repeatedly heated bloom in charcoal furnaces at 1200°C
Followed by working with a hammer
CO lead to the diffusion of C into the iron at the surface

Case Hardened Steel

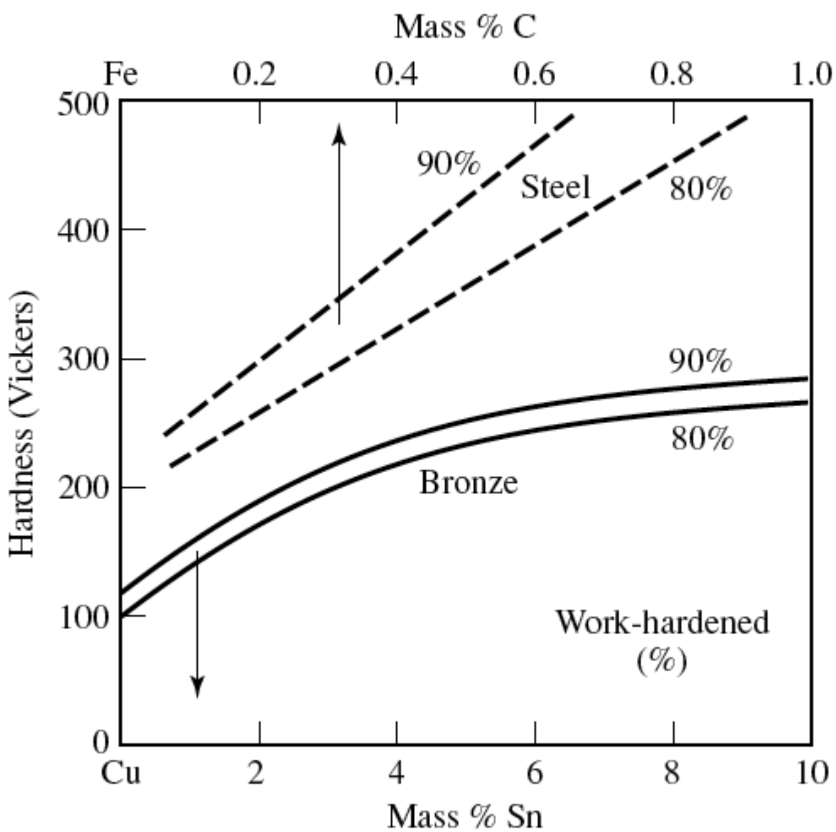

Even a fraction of a percent of carbon can have a dramatic effect on hardness

Hittites needed to beat bronze in terms of hardness so their weapons could pierce bronze shields

Quenching also hardened steel (Martensite)

(followed by tempering (heating))

Iron/Carbon Phase Diagram

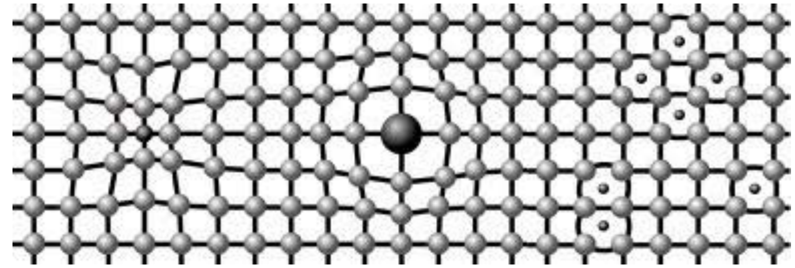

Iron shows a eutectic with Carbon allowing for a lower melting alloy

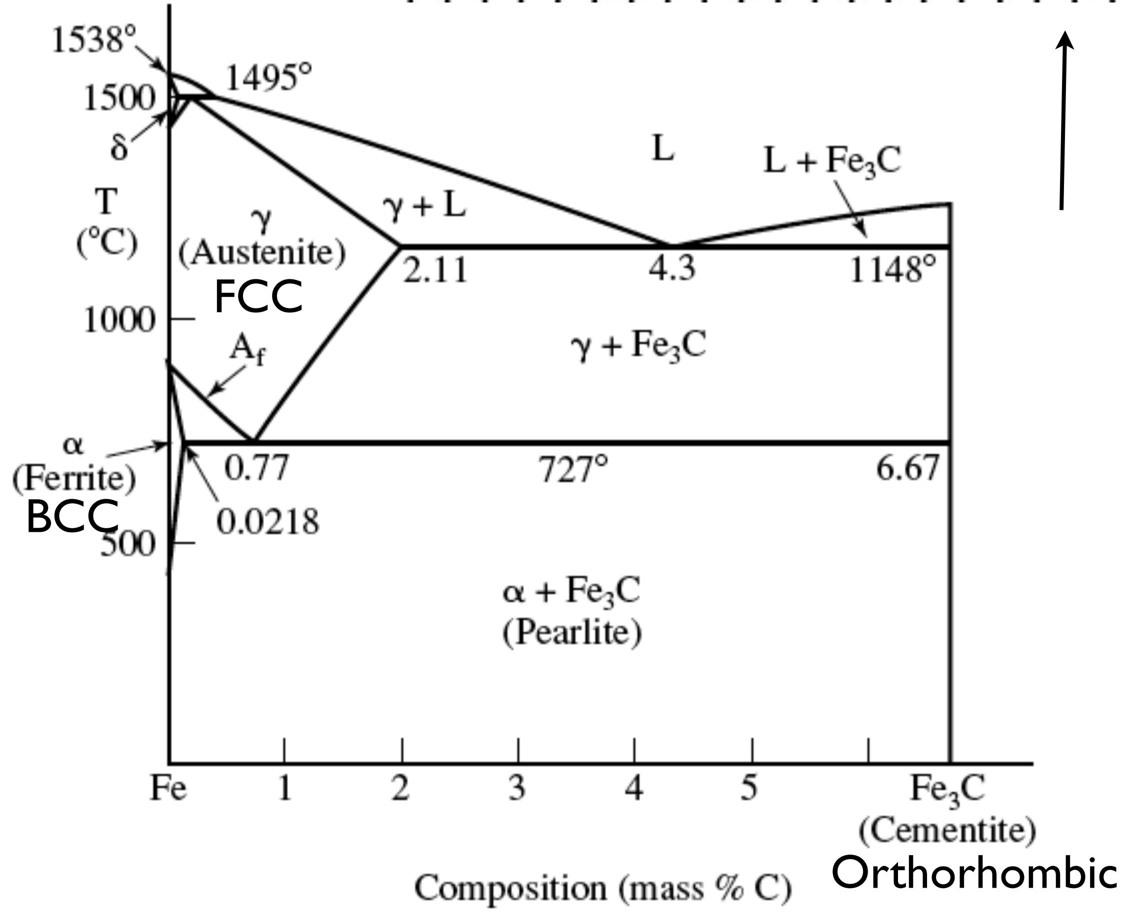

FIGURE 8.1. Portion of the iron–carbon phase diagram. (Actually, this section is known by the name *Fe-Fe_3C phase diagram*.) A_f is the highest temperature at which ferrite can form. As before, the mass percent of solute addition is used (formerly called weight percent).

Martensite (non equilibrium BCT phase from quench of γ)
Body Centered Tetragonal

Figure 11.2 The true equilibrium iron–carbon phase diagram with graphite instead of cementite as a stable phase. [Adapted from *Binary Alloy Phase Diagrams*, T. B. Massalski, (Editor-in-Chief), 1990. Reprinted by permission of ASM International, Materials Park, OH.]

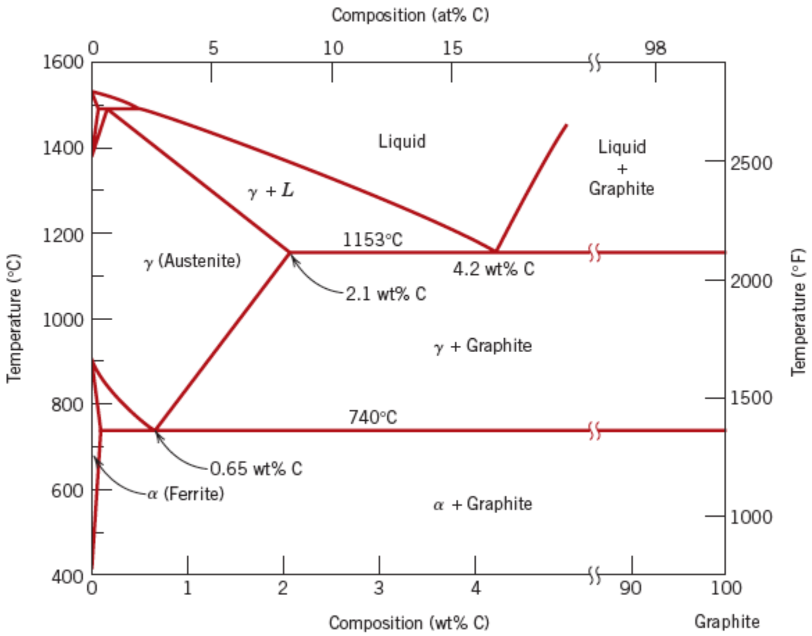

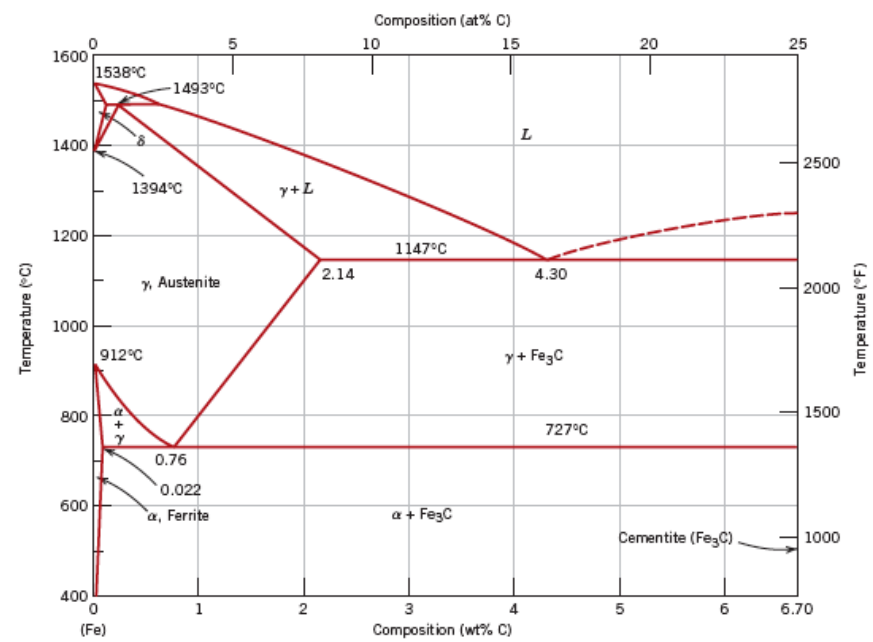

Figure 9.24 The iron–iron carbide phase diagram. [Adapted from *Binary Alloy Phase Diagrams*, 2nd edition, Vol. 1, T. B. Massalski (Editor-in-Chief), 1990. Reprinted by permission of ASM International, Materials Park, OH.]

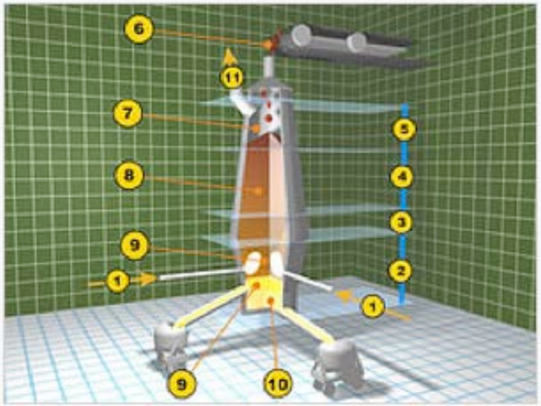

Blast furnace diagram

1. Hot blast from Cowper stoves
2. Melting zone (*bosh*)
3. Reduction zone of ferrous oxide (*barrel*)
4. Reduction zone of ferric oxide (*stack*)
5. Pre-heating zone (*throat*)
6. Feed of ore, limestone, and coke
7. Exhaust gases
8. Column of ore, coke and limestone
9. Removal of slag
10. Tapping of molten pig iron
11. Collection of waste gases

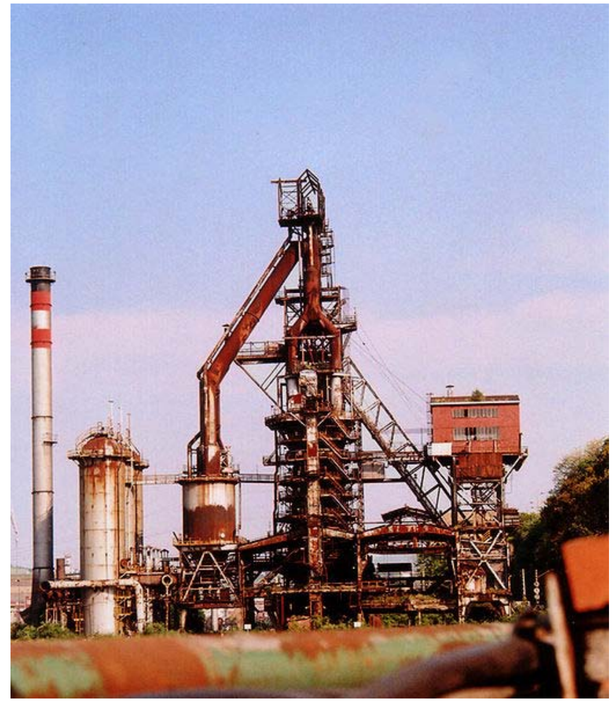

A **blast furnace** is a type of metallurgical furnace used for smelting to produce industrial metals, generally iron.

In a blast furnace, fuel and ore and flux (limestone) are continuously supplied through the top of the furnace, while air (sometimes with oxygen enrichment) is blown into the bottom of the chamber, so that the chemical reactions take place throughout the furnace as the material moves downward. The end products are usually molten metal and slag phases tapped from the bottom, and flue gases exiting from the top of the furnace. The downward flow of the ore and flux in contact with an upflow of hot combustion gases is a countercurrent exchange process.

Blast furnaces are to be contrasted with air furnaces (such as reverberatory furnaces), which were naturally aspirated, usually by the convection of hot gases in a chimney flue. According to this broad definition, bloomeries for iron, blowing houses for tin, and smelt mills for lead would be classified as blast furnaces. However, the term has usually been limited to those used for smelting iron ore to produce pig iron, an intermediate material used in the production of commercial iron and steel.

Pig iron is the intermediate product of smelting iron ore with a high-carbon fuel such as coke, usually with limestone as a flux. Charcoal and anthracite have also been used as fuel. Pig iron has a very high carbon content, typically 3.5–4.5%,[1] which makes it very brittle and not useful directly as a material except for limited applications.

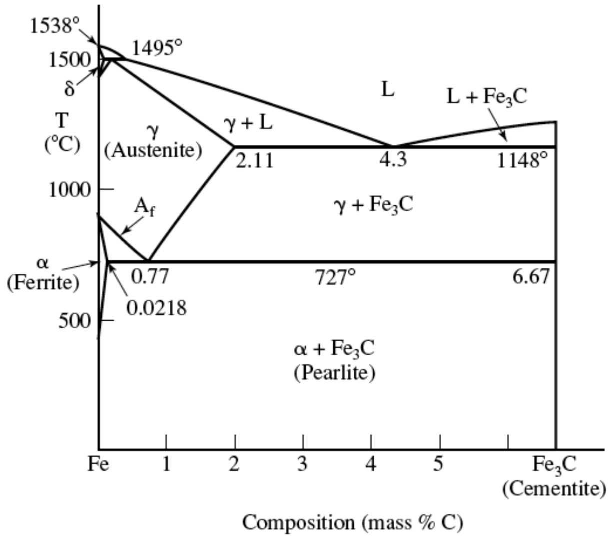

Carbon content can be reduced
by reaction with oxygen
and stirring

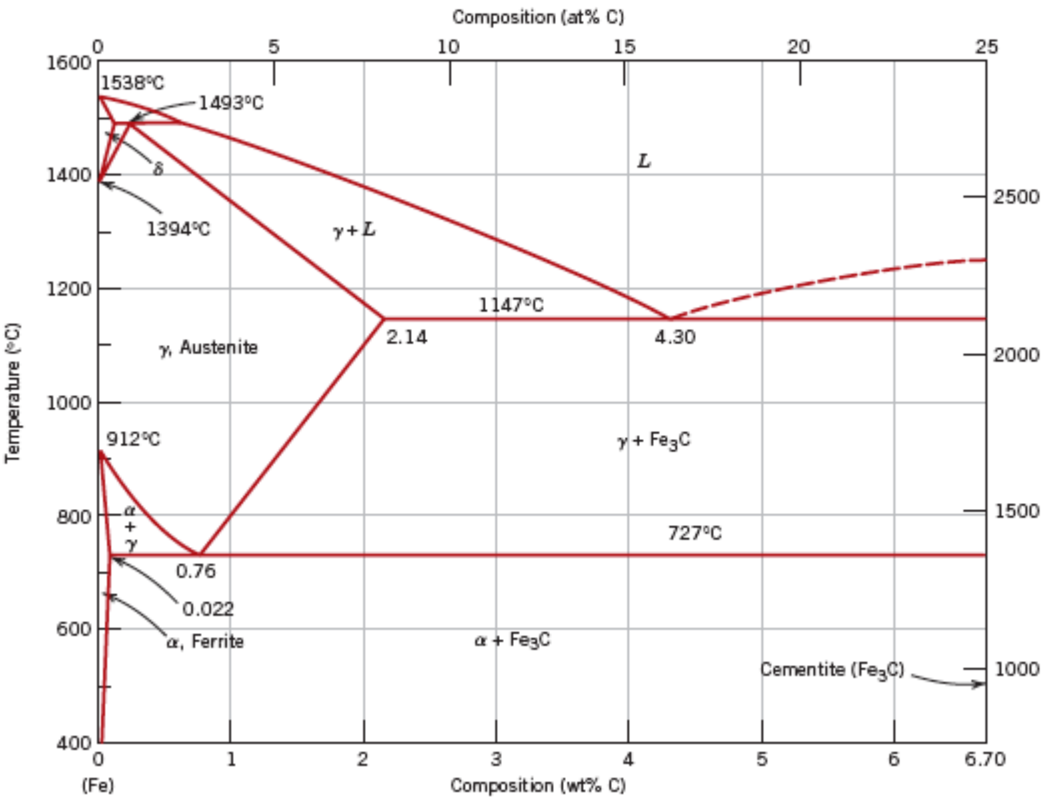

Figure 9.24 The iron–iron carbide phase diagram. [Adapted from *Binary Alloy Phase Diagrams,* 2nd edition, Vol. 1, T. B. Massalski (Editor-in-Chief), 1990. Reprinted by permission of ASM International, Materials Park, OH.]

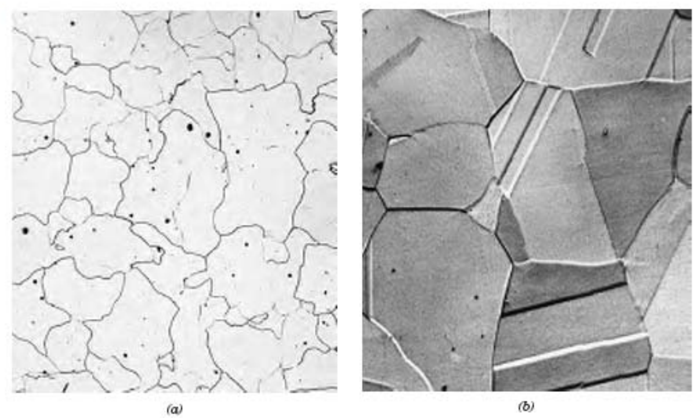

Figure 9.25 Photomicrographs of (*a*) α ferrite (90×) and (*b*) austenite (325×). (Copyright 1971 by United States Steel Corporation.)

Eutectoid Steel Pearlite

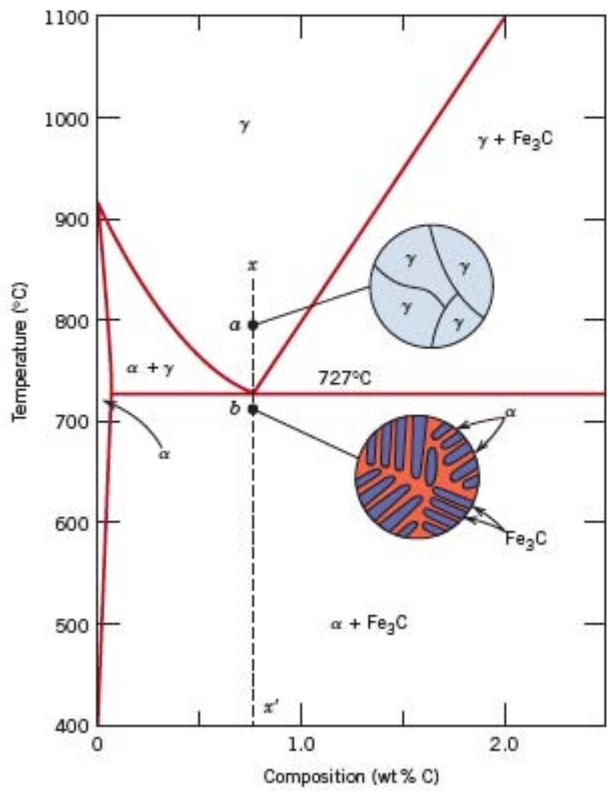

Figure 9.26 Schematic representations of the microstructures for an iron–carbon alloy of eutectoid composition (0.76 wt% C) above and below the eutectoid temperature.

FIGURE 8.2. Schematic representation of a lamellar (plate-like) microstructure of steel called pearlite obtained by cooling a eutectoid iron–carbon alloy from austenite to below 727°C. Pearlite is a mixture of α and Fe_3C. Compare to Figure 5.9.

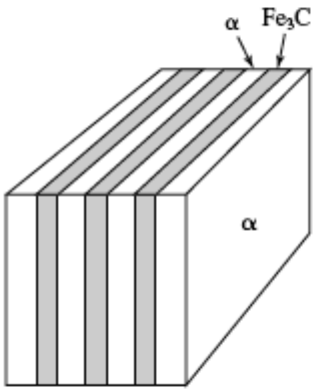

Figure 9.27 Photomicrograph of a eutectoid steel showing the pearlite microstructure consisting of alternating layers of α ferrite (the light phase) and Fe_3C (thin layers most of which appear dark). 500×. (Reproduced with permission from *Metals Handbook,* 9th edition, Vol. 9, *Metallography and Microstructures,* American Society for Metals, Materials Park, OH, 1985.)

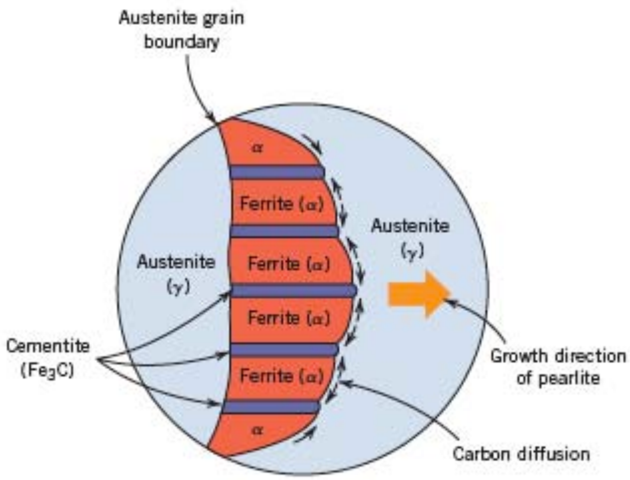

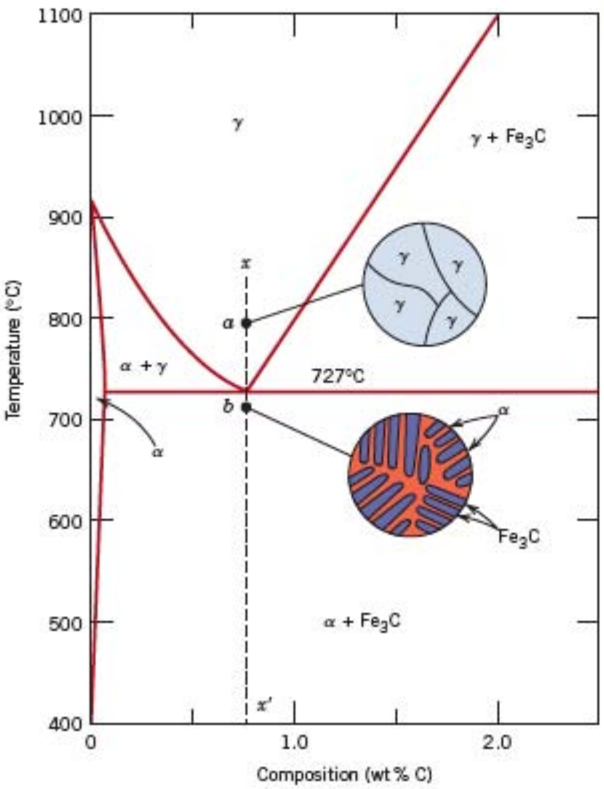

Figure 9.26 Schematic representations of the microstructures for an iron–carbon alloy of eutectoid composition (0.76 wt% C) above and below the eutectoid temperature.

Time-Temperature-Transformation Diagram

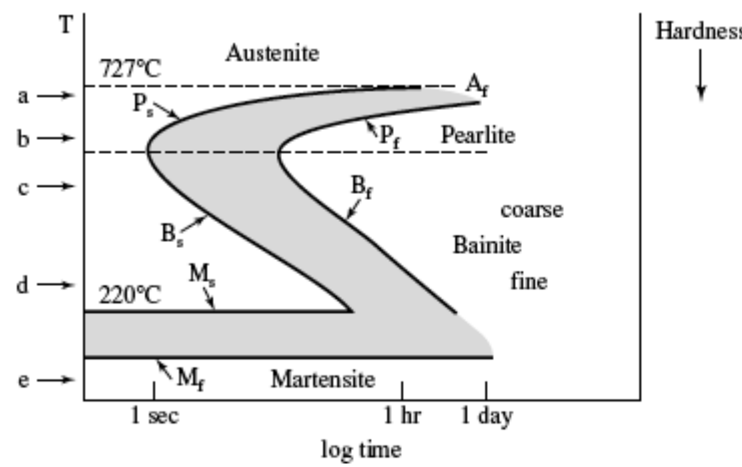

FIGURE 8.4. Schematic representation of a TTT diagram for eutectoid steel. The annealing temperatures (a) through (e) refer to specific cases as described in the text. Note that the hardness scale on the right points downward.

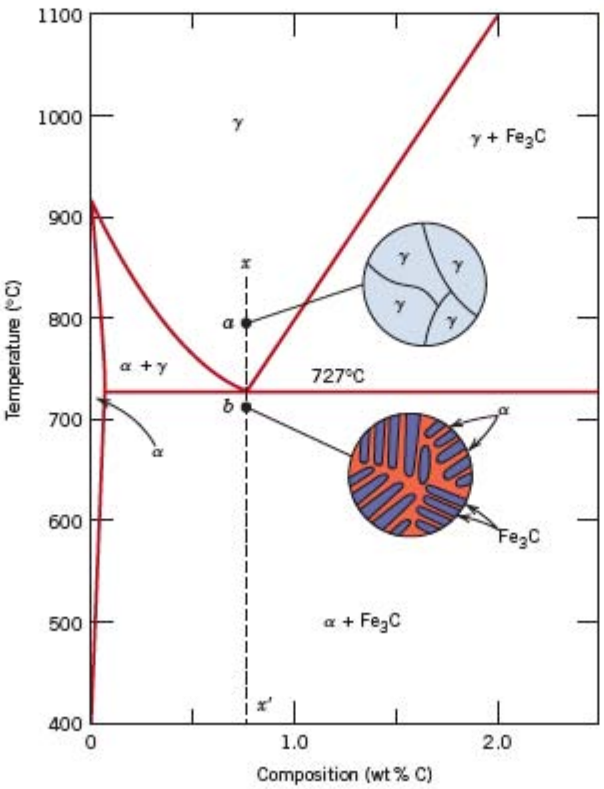

Figure 9.26 Schematic representations of the microstructures for an iron–carbon alloy of eutectoid composition (0.76 wt% C) above and below the eutectoid temperature.

Time-Temperature-Transformation Diagram

Just below 727°C
Thermodynamics drive is low
so time is long

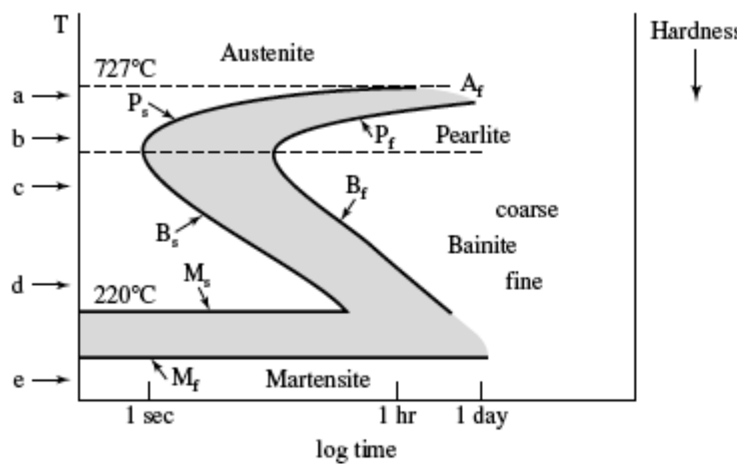

FIGURE 8.4. Schematic representation of a TTT diagram for eutectoid steel. The annealing temperatures (a) through (e) refer to specific cases as described in the text. Note that the hardness scale on the right points downward.

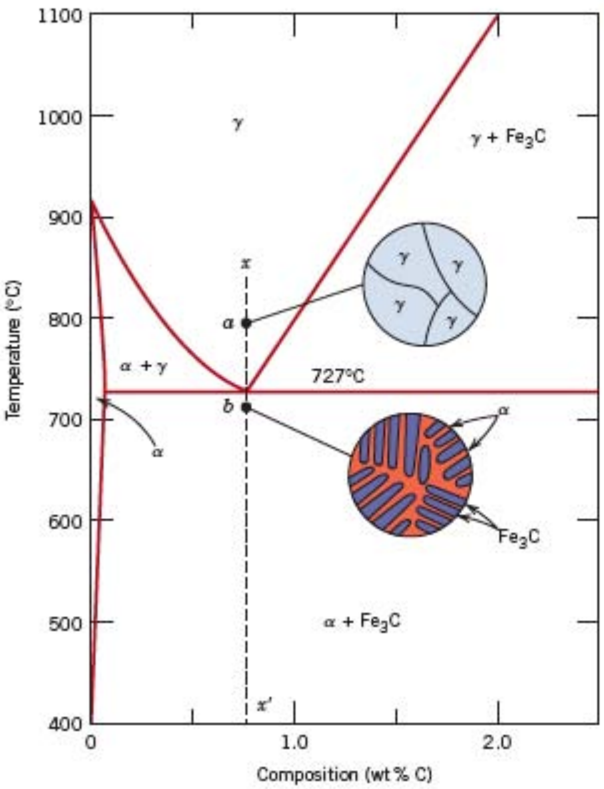

Figure 9.26 Schematic representations of the microstructures for an iron–carbon alloy of eutectoid composition (0.76 wt% C) above and below the eutectoid temperature.

Time-Temperature-Transformation Diagram

Well below 727°C
Diffusion is slow
so time is long

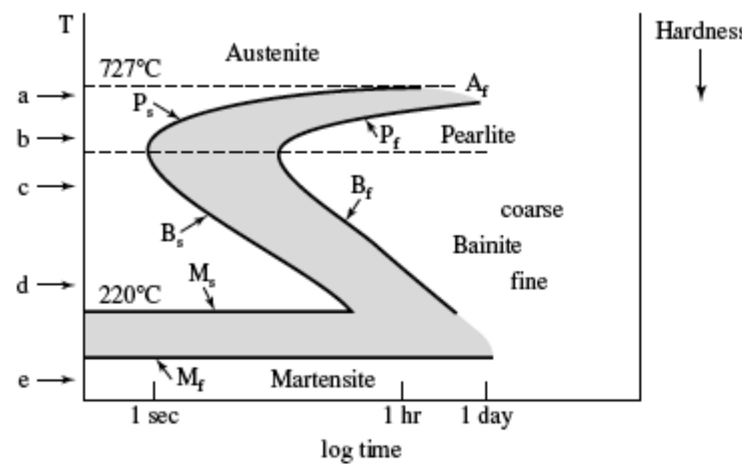

FIGURE 8.4. Schematic representation of a TTT diagram for eutectoid steel. The annealing temperatures (a) through (e) refer to specific cases as described in the text. Note that the hardness scale on the right points downward.

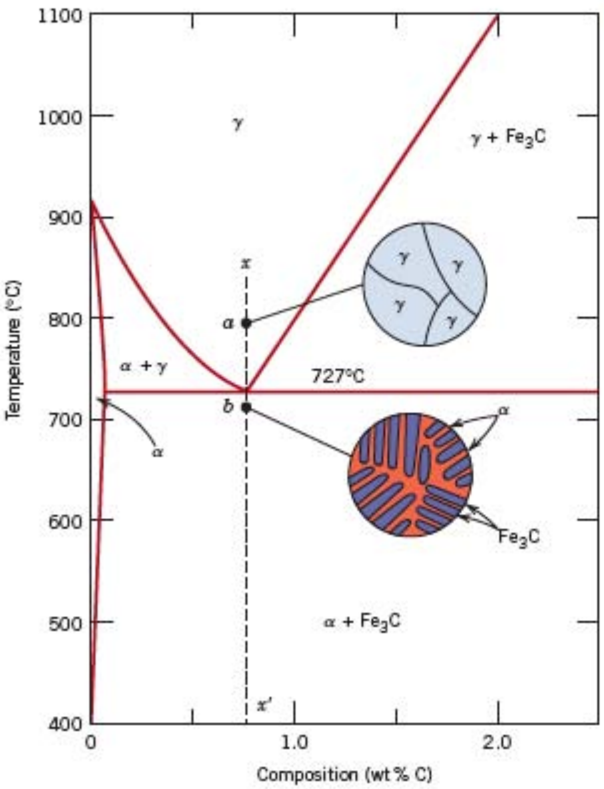

Figure 9.26 Schematic representations of the microstructures for an iron–carbon alloy of eutectoid composition (0.76 wt% C) above and below the eutectoid temperature.

Time-Temperature-Transformation Diagram

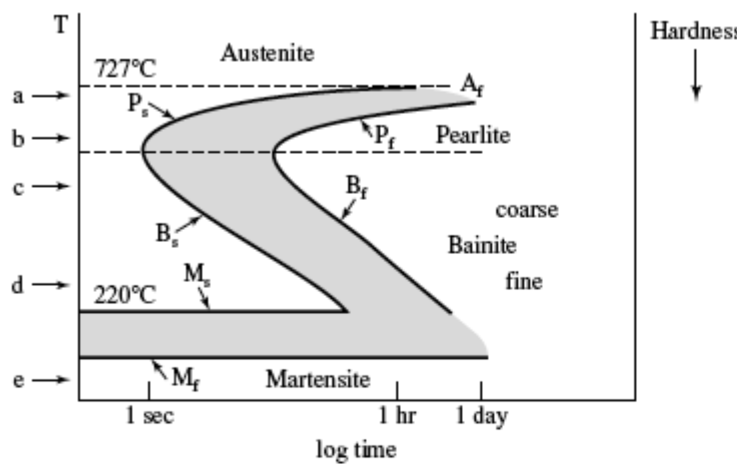

FIGURE 8.4. Schematic representation of a TTT diagram for eutectoid steel. The annealing temperatures (a) through (e) refer to specific cases as described in the text. Note that the hardness scale on the right points downward.

At very deep quenches Diffusionless Transformation Occurs: Martinsitic Transformation

Hypoeutectoid Steel

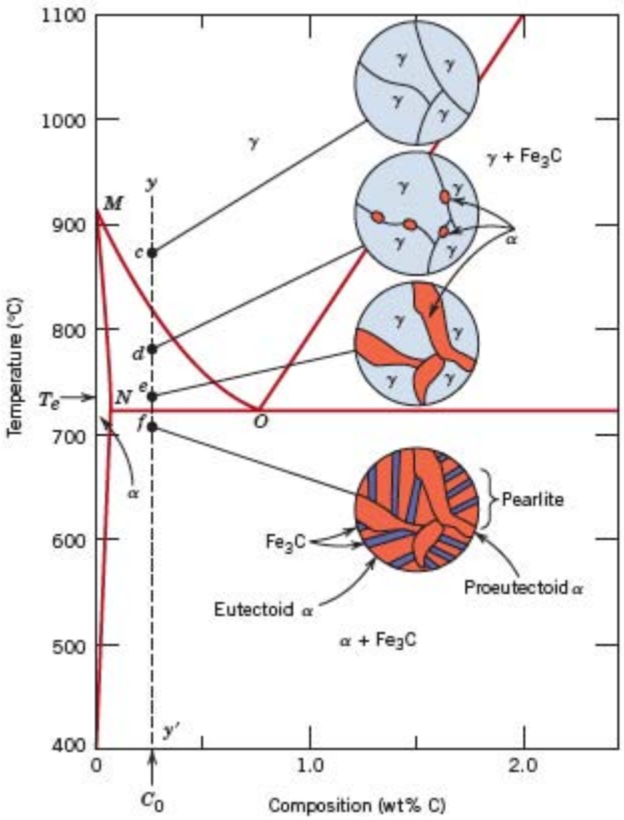

Figure 9.29 Schematic representations of the microstructures for an iron–carbon alloy of hypoeutectoid composition C_0 (containing less than 0.76 wt% C) as it is cooled from within the austenite phase region to below the eutectoid temperature.

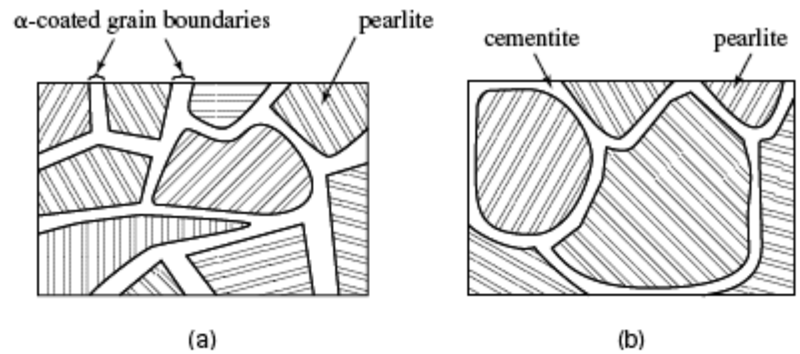

FIGURE 8.3. Schematic representation of (a) a *hypo*eutectoid microstructure of steel at room temperature containing primary α and pearlite microconstituents (the latter consisting of two phases, i.e., α and Fe_3C); (b) a *hyper*eutectoid microstructure of steel. Note that the primary phases in both cases have "coated" the former grain boundaries of the austenite.

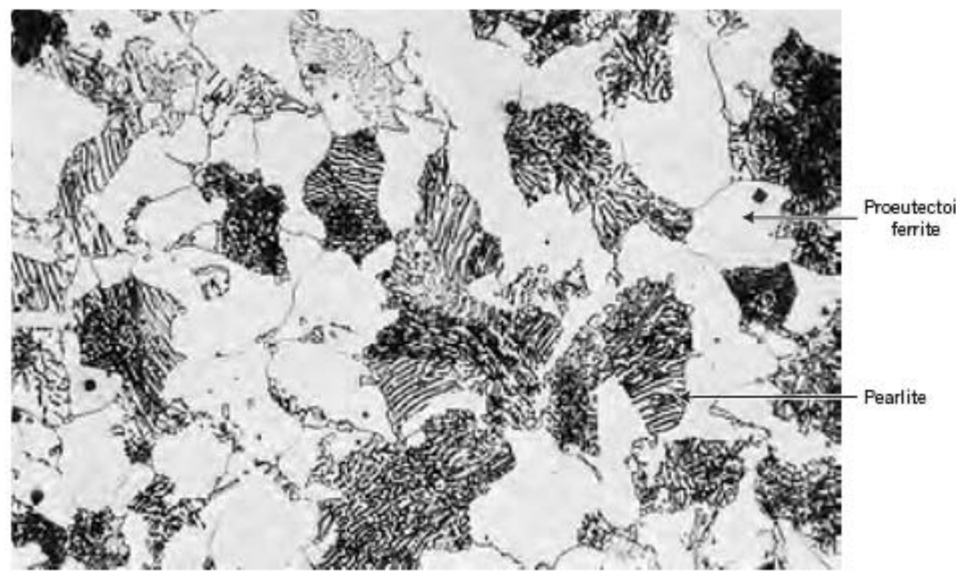

Figure 9.30 Photomicrograph of a 0.38 wt% C steel having a microstructure consisting of pearlite and proeutectoid ferrite. 635×. (Photomicrograph courtesy of Republic Steel Corporation.)

Hypoeutectoid Steel

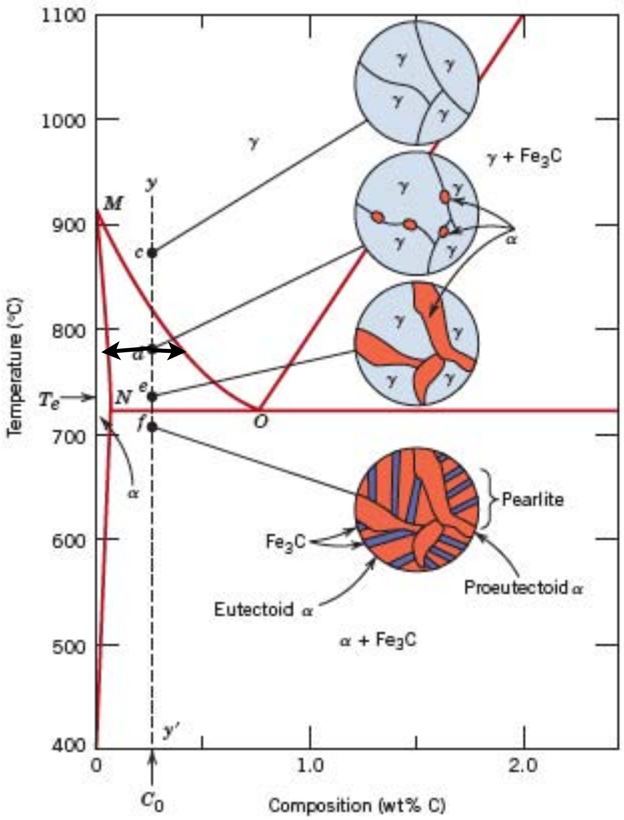

Figure 9.29 Schematic representations of the microstructures for an iron–carbon alloy of hypoeutectoid composition C_0 (containing less than 0.76 wt% C) as it is cooled from within the austenite phase region to below the eutectoid temperature.

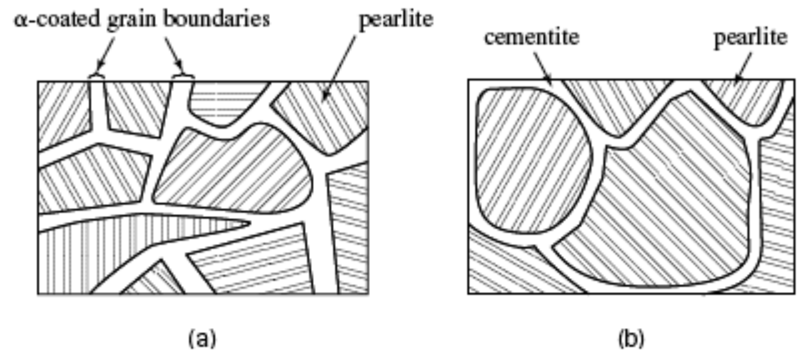

FIGURE 8.3. Schematic representation of (a) a *hypo*eutectoid microstructure of steel at room temperature containing primary α and pearlite microconstituents (the latter consisting of two phases, i.e., α and Fe_3C); (b) a *hyper*eutectoid microstructure of steel. Note that the primary phases in both cases have "coated" the former grain boundaries of the austenite.

Figure 9.30 Photomicrograph of a 0.38 wt% C steel having a microstructure consisting of pearlite and proeutectoid ferrite. 635×. (Photomicrograph courtesy of Republic Steel Corporation.)

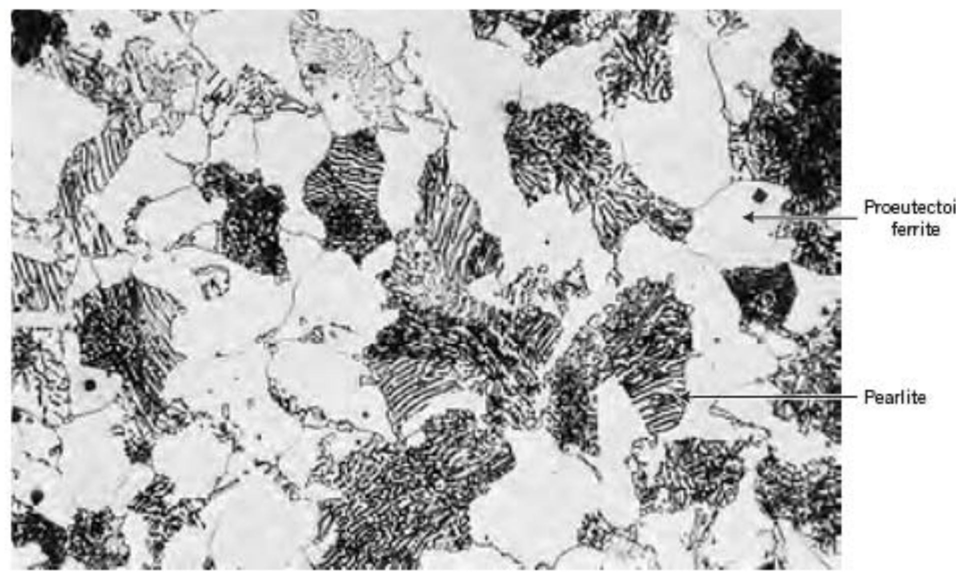

Hypoeutectoid Steel

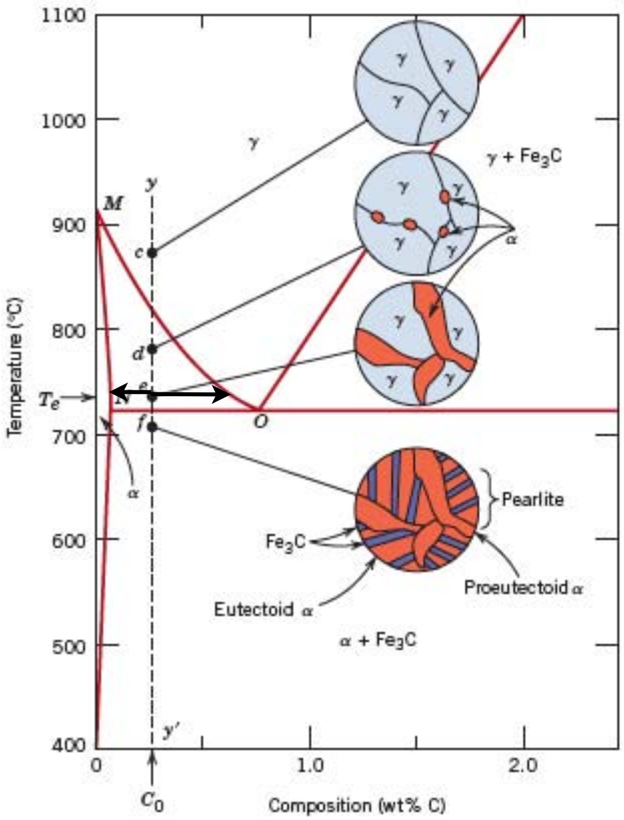

Figure 9.29 Schematic representations of the microstructures for an iron–carbon alloy of hypoeutectoid composition C_0 (containing less than 0.76 wt% C) as it is cooled from within the austenite phase region to below the eutectoid temperature.

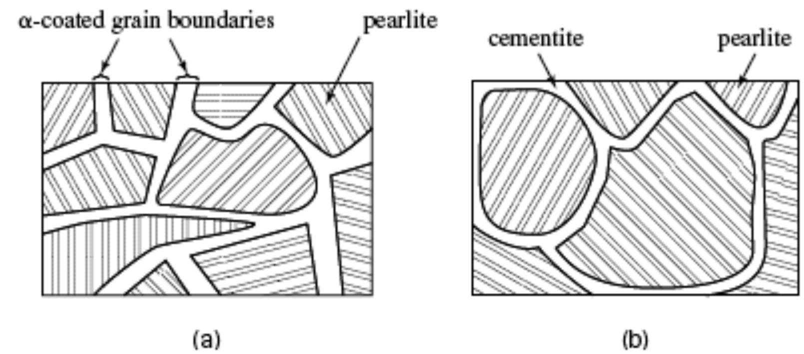

FIGURE 8.3. Schematic representation of (a) a *hypo*eutectoid microstructure of steel at room temperature containing primary α and pearlite microconstituents (the latter consisting of two phases, i.e., α and Fe_3C); (b) a *hyper*eutectoid microstructure of steel. Note that the primary phases in both cases have "coated" the former grain boundaries of the austenite.

Figure 9.30 Photomicrograph of a 0.38 wt% C steel having a microstructure consisting of pearlite and proeutectoid ferrite. 635×. (Photomicrograph courtesy of Republic Steel Corporation.)

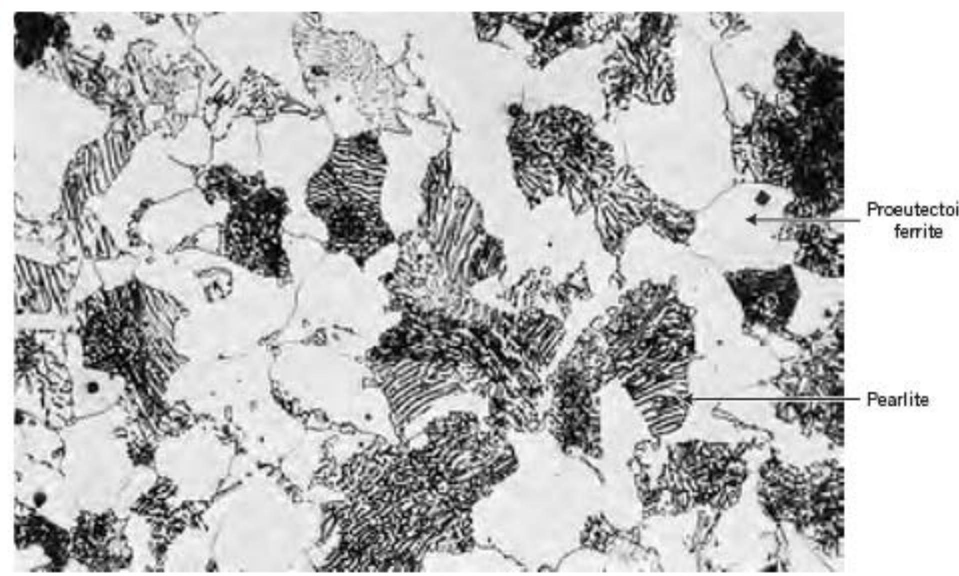

Hypoeutectoid Steel

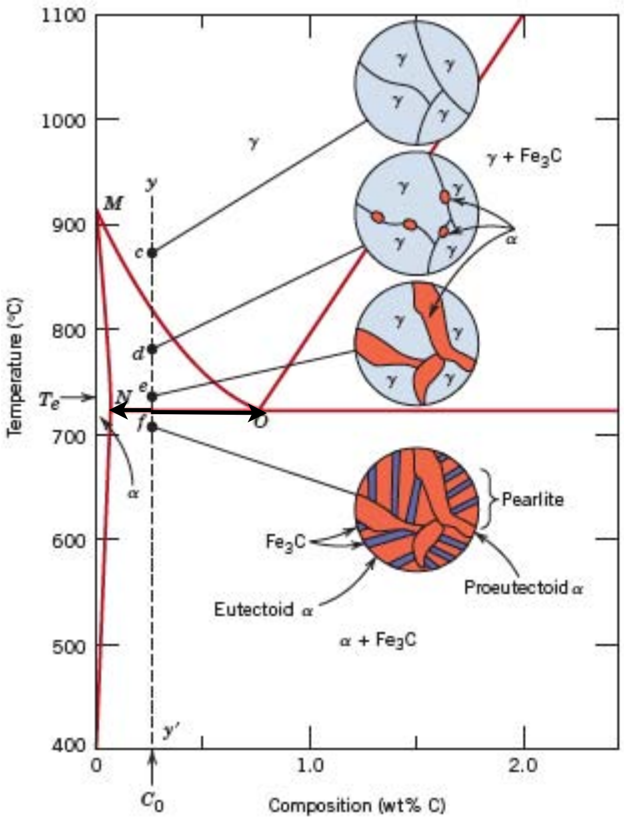

Figure 9.29 Schematic representations of the microstructures for an iron–carbon alloy of hypoeutectoid composition C_0 (containing less than 0.76 wt% C) as it is cooled from within the austenite phase region to below the eutectoid temperature.

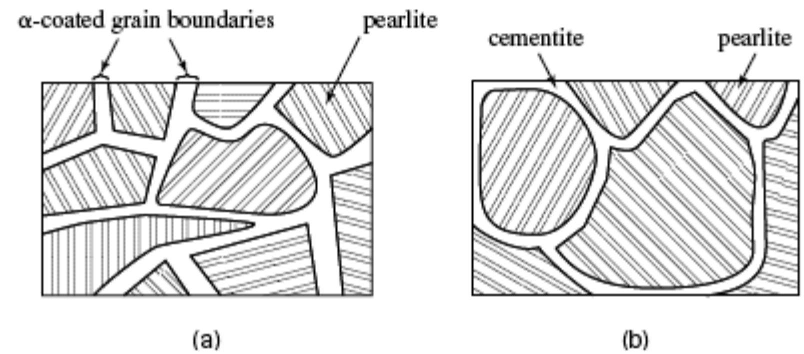

FIGURE 8.3. Schematic representation of (a) a *hypo*eutectoid microstructure of steel at room temperature containing primary α and pearlite microconstituents (the latter consisting of two phases, i.e., α and Fe_3C); (b) a *hyper*eutectoid microstructure of steel. Note that the primary phases in both cases have "coated" the former grain boundaries of the austenite.

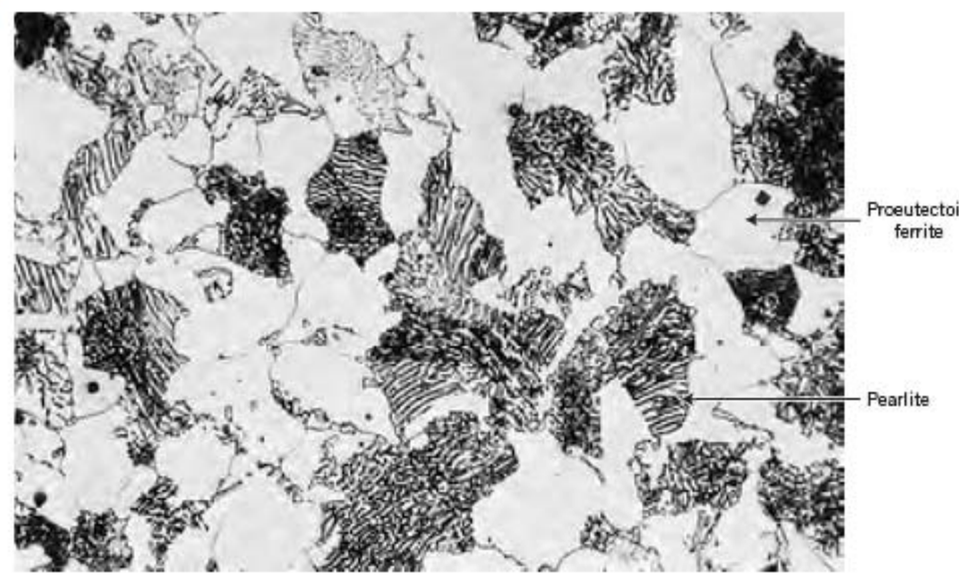

Figure 9.30 Photomicrograph of a 0.38 wt% C steel having a microstructure consisting of pearlite and proeutectoid ferrite. 635×. (Photomicrograph courtesy of Republic Steel Corporation.)

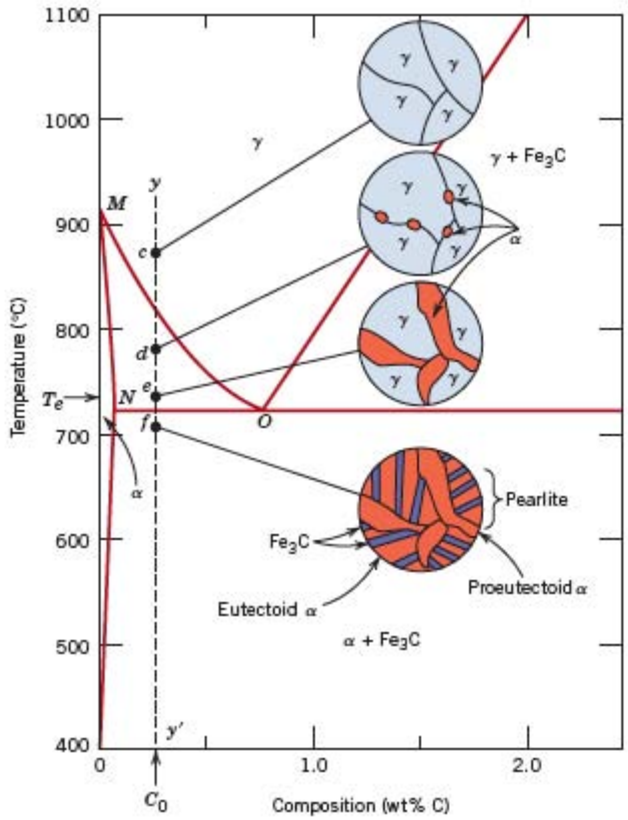

Figure 9.29 Schematic representations of the microstructures for an iron–carbon alloy of hypoeutectoid composition C_0 (containing less than 0.76 wt% C) as it is cooled from within the austenite phase region to below the eutectoid temperature.

FIGURE 8.5. Schematic representation of a TTT diagram for a hypoeutectoid plain carbon steel. A_f is the highest temperature at which ferrite can form; see Figure 8.1. F_s is the ferrite start temperature.

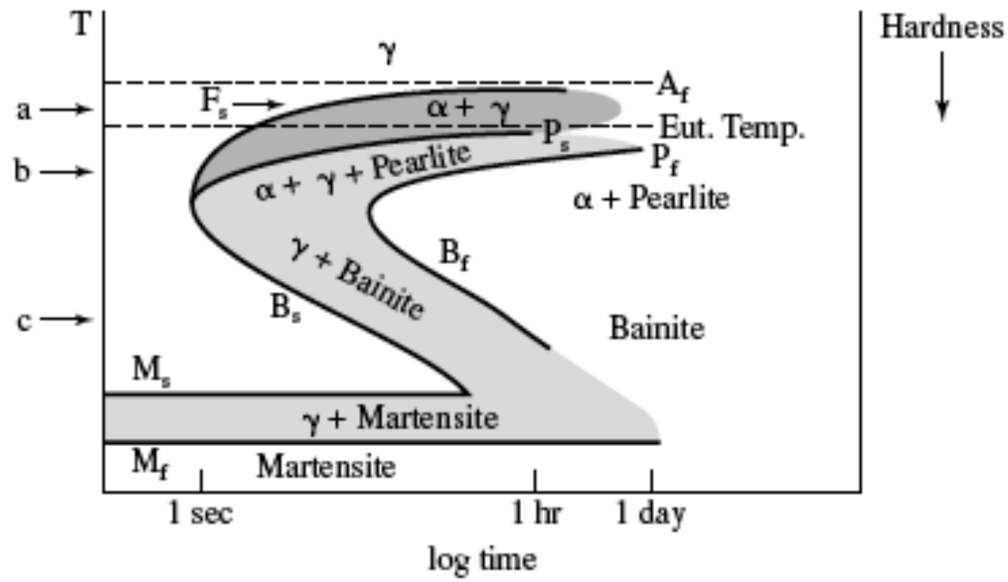

Hypereutectoid Steel

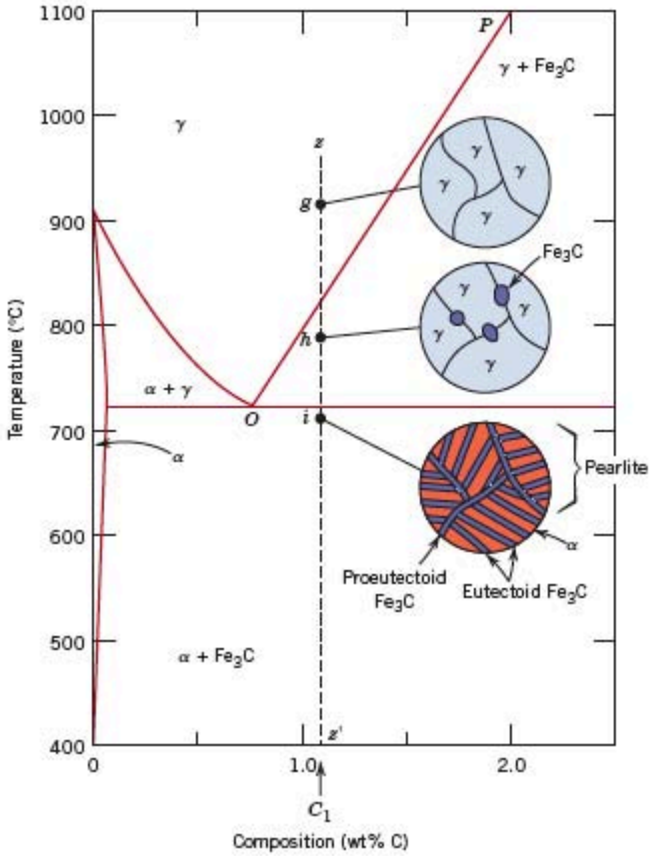

Figure 9.32 Schematic representations of the microstructures for an iron–carbon alloy of hypereutectoid composition C_1 (containing between 0.76 and 2.14 wt% C), as it is cooled from within the austenite phase region to below the eutectoid temperature.

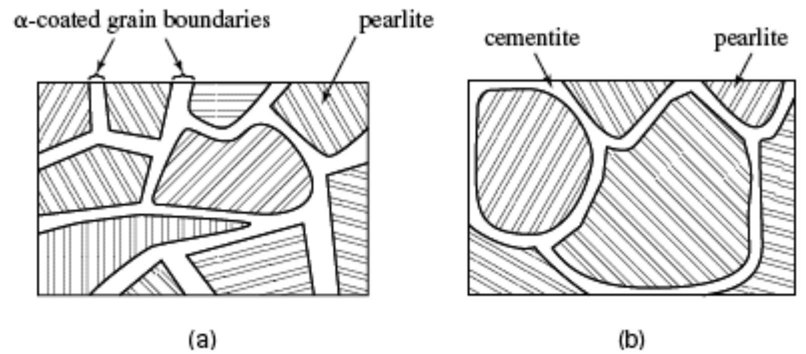

FIGURE 8.3. Schematic representation of (a) a *hypo*eutectoid microstructure of steel at room temperature containing primary α and pearlite microconstituents (the latter consisting of two phases, i.e., α and Fe_3C); (b) a *hyper*eutectoid microstructure of steel. Note that the primary phases in both cases have "coated" the former grain boundaries of the austenite.

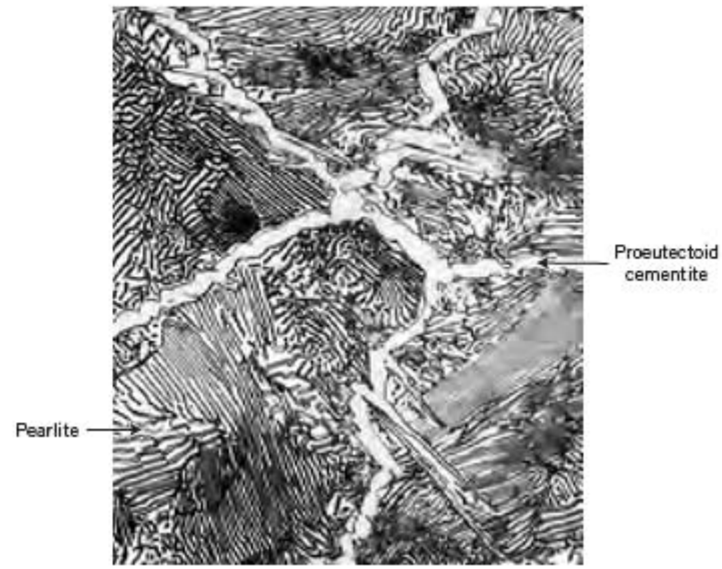

Figure 9.33 Photomicrograph of a 1.4 wt% C steel having a microstructure consisting of a white proeutectoid cementite network surrounding the pearlite colonies. 1000×. (Copyright 1971 by United States Steel Corporation.)

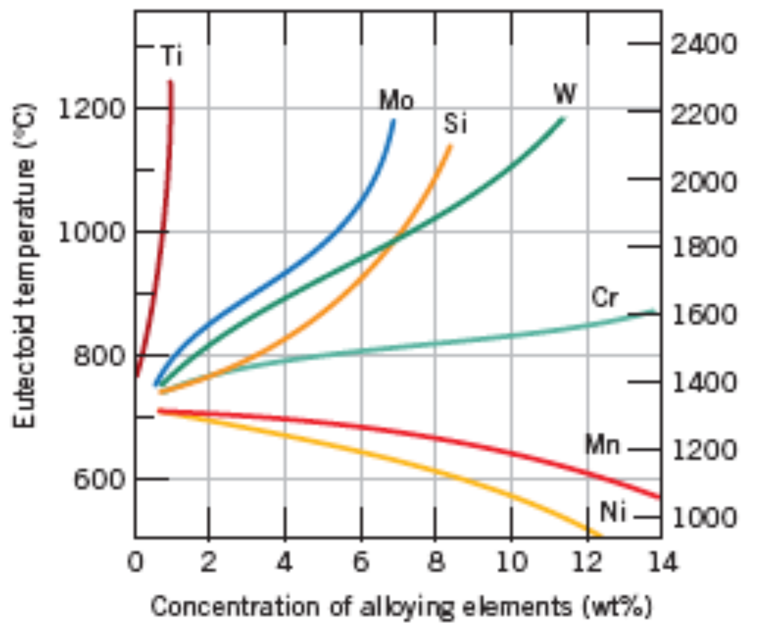

Figure 9.34 The dependence of eutectoid temperature on alloy concentration for several alloying elements in steel. (From Edgar C. Bain, *Functions of the Alloying Elements in Steel,* American Society for Metals, 1939, p. 127.)

Kinetics of Phase Growth

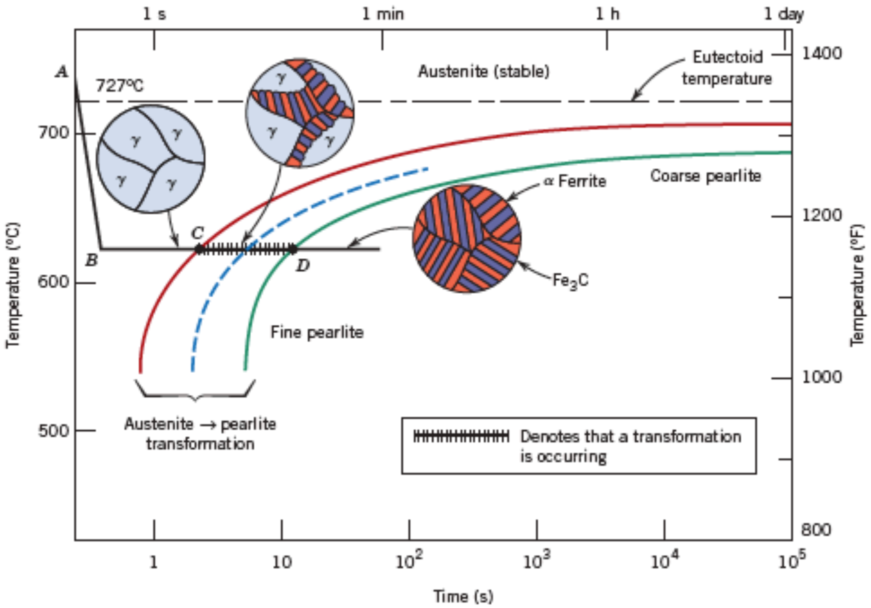

Figure 10.14 Isothermal transformation diagram for a eutectoid iron–carbon alloy, with superimposed isothermal heat treatment curve (*ABCD*). Microstructures before, during, and after the austenite-to-pearlite transformation are shown. [Adapted from H. Boyer (Editor), *Atlas of Isothermal Transformation and Cooling Transformation Diagrams,* American Society for Metals, 1977, p. 28.]

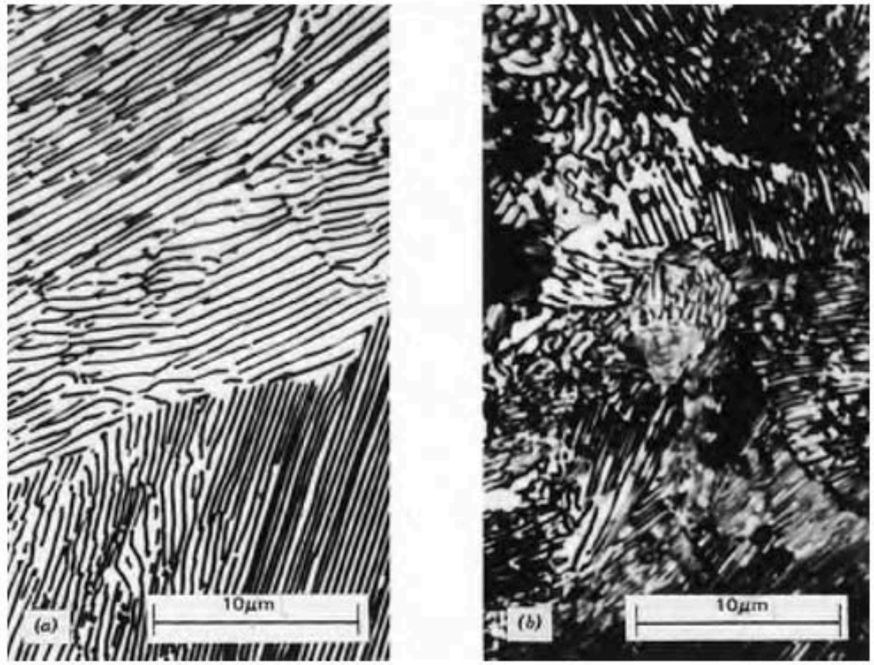

Figure 10.15 Photomicrographs of (*a*) coarse pearlite and (*b*) fine pearlite. 3000×. (From K. M. Ralls et al., *An Introduction to Materials Science and Engineering,* p. 361. Copyright © 1976 by John Wiley & Sons, New York. Reprinted by permission of John Wiley & Sons, Inc.)

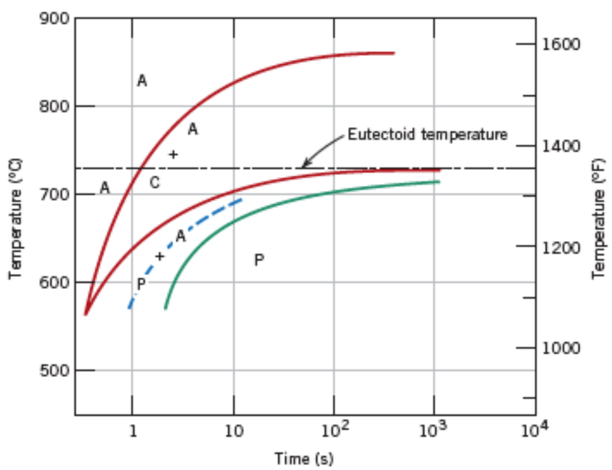

Figure 10.16 Isothermal transformation diagram for a 1.13 wt% C iron–carbon alloy: A, austenite; C, proeutectoid cementite; P, pearlite. [Adapted from H. Boyer (Editor), *Atlas of Isothermal Transformation and Cooling Transformation Diagrams,* American Society for Metals, 1977, p. 33.]

Figure 10.17 Transmission electron micrograph showing the structure of bainite. A grain of bainite passes from lower left to upper right-hand corners, which consists of elongated and needle-shaped particles of Fe_3C within a ferrite matrix. The phase surrounding the bainite is martensite. (Reproduced with permission from *Metals Handbook,* 8th edition, Vol. 8, *Metallography, Structures and Phase Diagrams,* American Society for Metals, Materials Park, OH, 1973.)

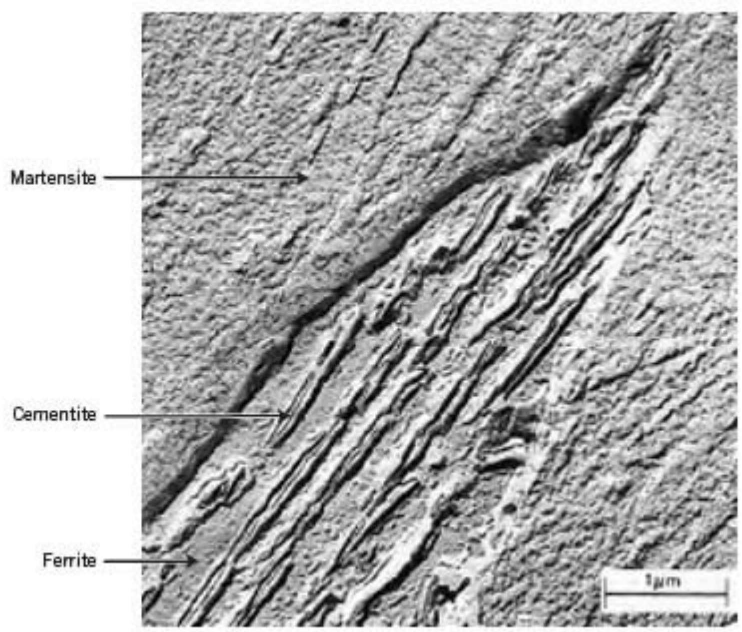

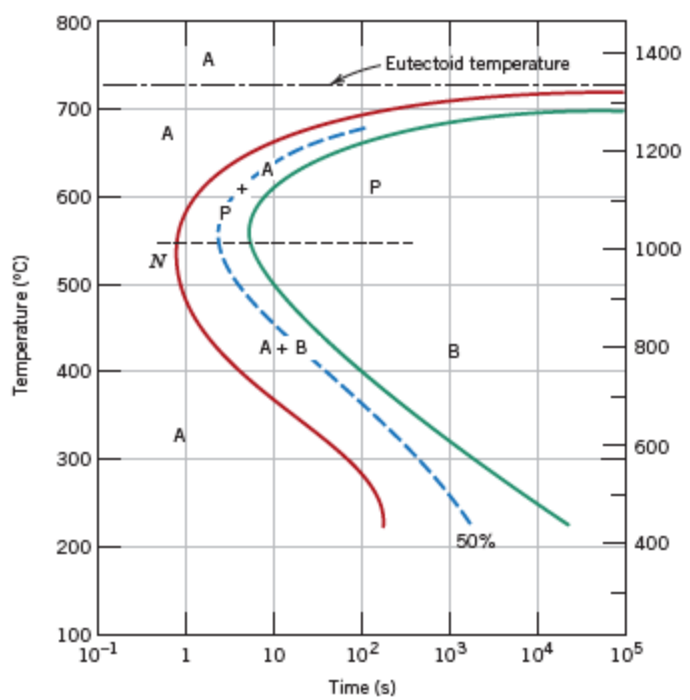

Figure 10.18 Isothermal transformation diagra for an iron–carbon alloy of eutectoid composition, includin austenite-to-pearlite (A–P) and austenite-to-bainite (A–B) transformations. [Adapted from H. Boyer (Editor), *Atlas of Isothermal Transformation and Cooling Transformation Diagrams,* American Society for Metals, 1977, p. 28.]

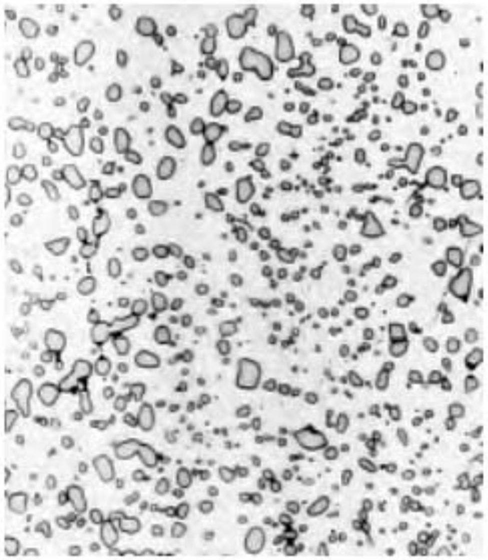

Figure 10.19 Photomicrograph of a steel having a spheroidite microstructure. The small particles are cementite; the continuous phase is α ferrite. 1000×. (Copyright 1971 by United States Steel Corporation.)

Heat Treatment of Steel

Quench and tempering: This is the most common heat treatment encountered, because the final properties can be precisely determined by the temperature and time of the tempering. Tempering involves reheating quenched steel to a temperature below the eutectoid temperature then cooling. The elevated temperature allows very small amounts of spheroidite to form, which restores ductility, but reduces hardness. Actual temperatures and times are carefully chosen for each composition.

Spheroidizing: Spheroidite forms when carbon steel is heated to approximately 700 °C for over 30 hours. Spheroidite can form at lower temperatures but the time needed drastically increases, as this is a diffusion-controlled process. The result is a structure of rods or spheres of cementite within primary structure (ferrite or pearlite, depending on which side of the eutectoid you are on). The purpose is to soften higher carbon steels and allow more formability. This is the softest and most ductile form of steel.

Process annealing: A process used to relieve stress in a cold-worked carbon steel with less than 0.3 wt% C. The steel is usually heated up to 550–650 °C for 1 hour, but sometimes temperatures as high as 700 °C.

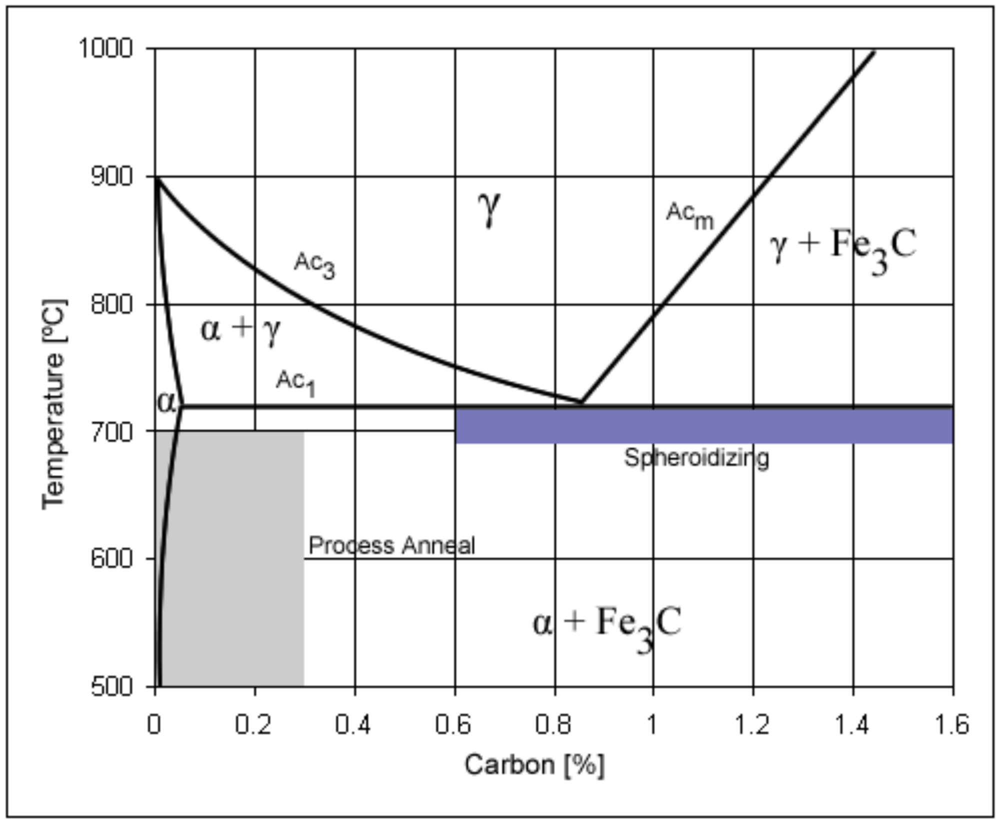

Martensite

Austinite => Martensite Transformation
FCC => BCT

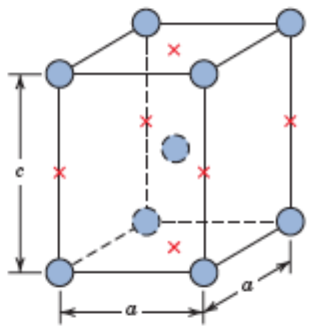

Figure 10.20 The body-centered tetragonal unit cell for martensitic steel showing iron atoms (circles) and sites that may be occupied by carbon atoms (crosses). For this tetragonal unit cell, $c > a$.

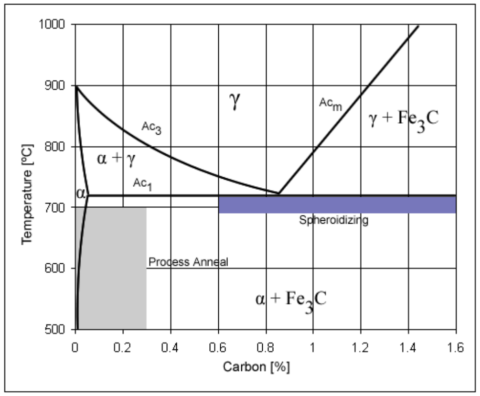

Figure 10.21 Photomicrograph showing the martensitic microstructure. The needle-shaped grains are the martensite phase, and the white regions are austenite that failed to transform during the rapid quench. 1220×. (Photomicrograph courtesy of United States Steel Corporation.)

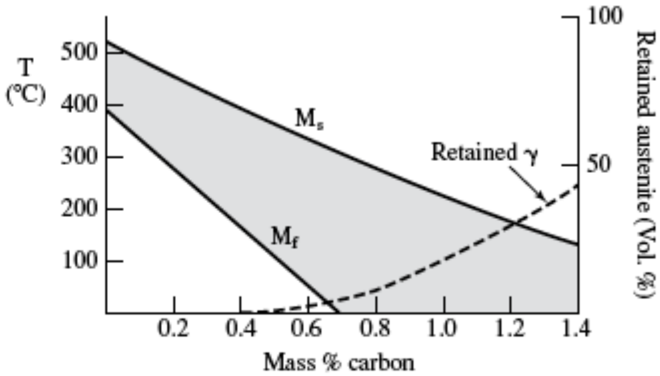

FIGURE 8.6. Schematic representation of the influence of carbon concentration on the M_s and M_f temperatures in steel and on the amount of retained austenite (given in volume percent).

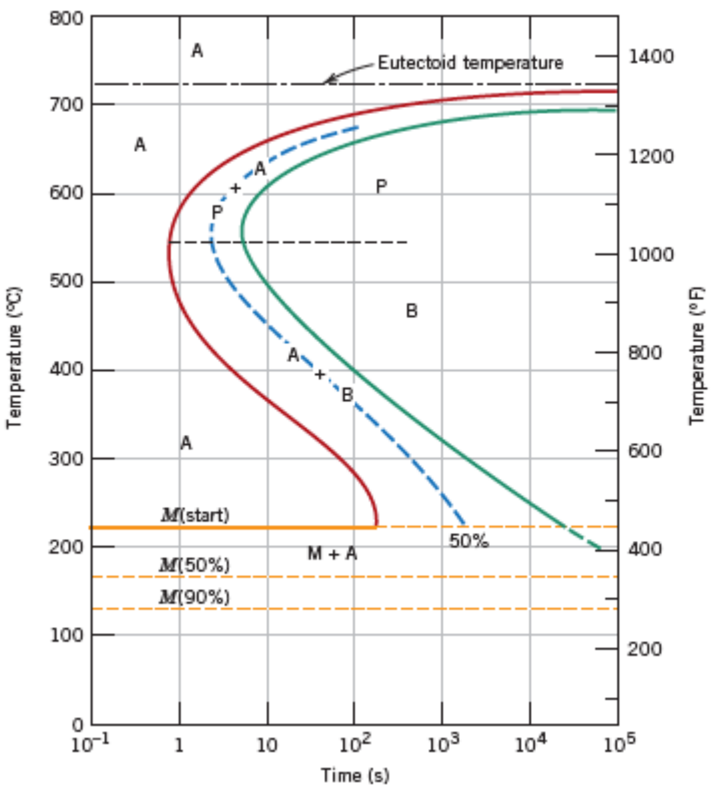

Figure 10.22 The complete isothermal transformation diagram for an iron–carbon alloy of eutectoid composition: A, austenite; B, bainite; M, martensite; P, pearlite.

Figure 10.23 Isothermal transformation diagram for an alloy steel (type 4340): A, austenite; B, bainite; P, pearlite; M, martensite; F, proeutectoid ferrite. [Adapted from H. Boyer (Editor), *Atlas of Isothermal Transformation and Cooling Transformation Diagrams*, American Society for Metals, 1977, p. 181.]

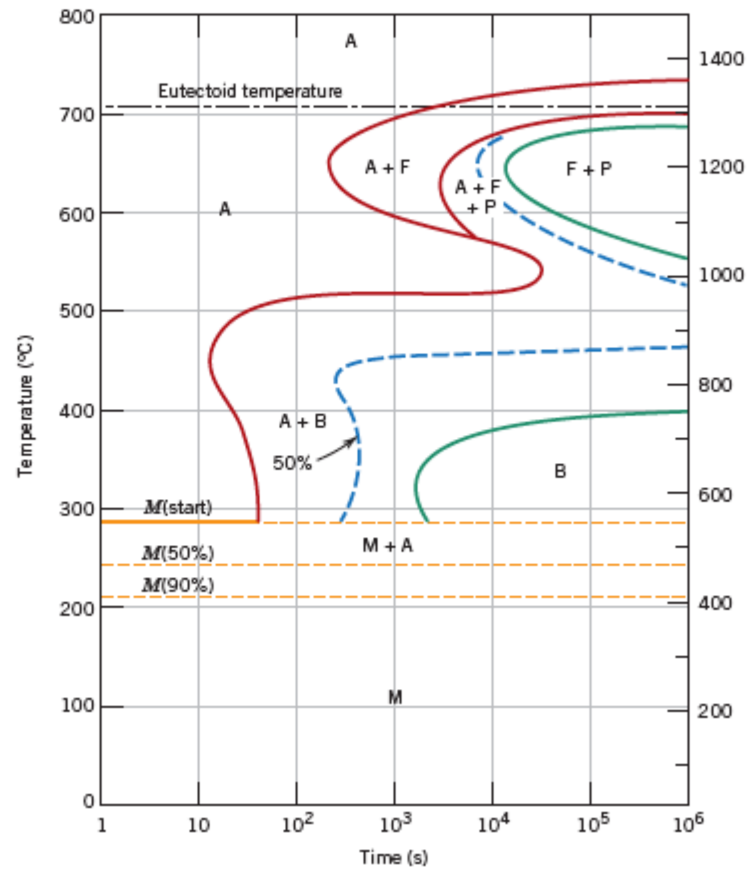

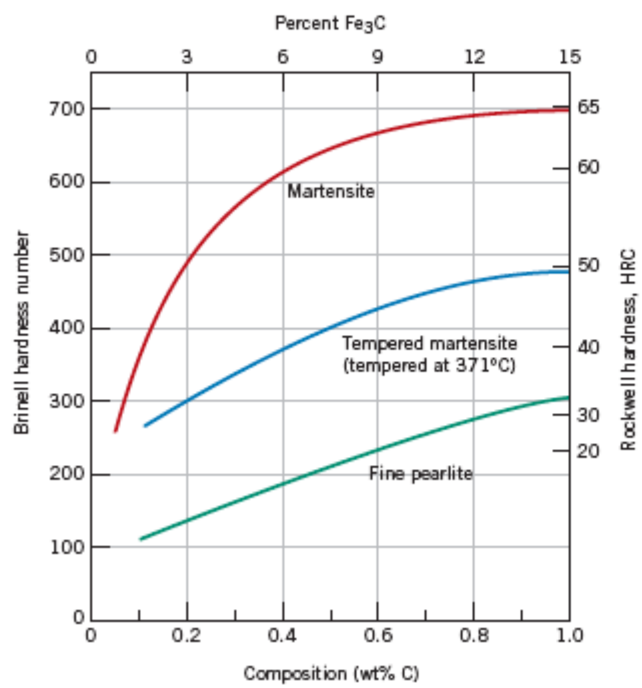

Figure 10.32 Hardness (at room temperature) as a function of carbon concentration for plain carbon martensitic, tempered martensitic [tempered at 371°C (700°F)], and pearlitic steels. (Adapted from Edgar C. Bain, *Functions of the Alloying Elements in Steel,* American Society for Metals, 1939, p. 36; and R. A. Grange, C. R. Hribal, and L. F. Porter, *Metall. Trans. A,* Vol. 8A, p. 1776.)

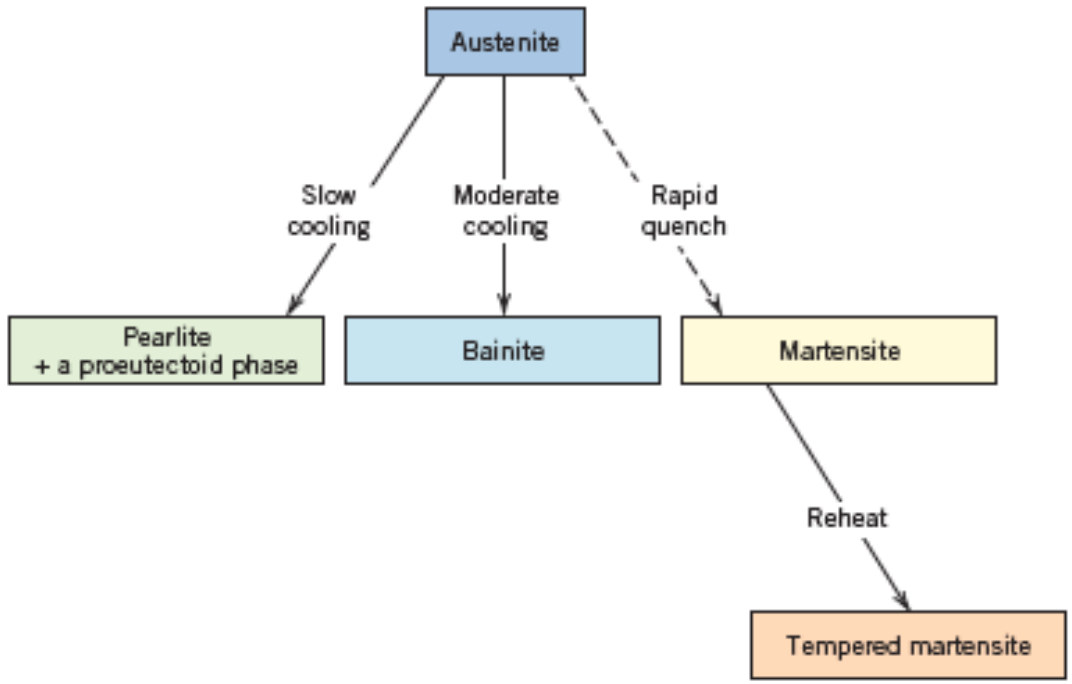

Figure 10.36 Possible transformations involving the decomposition of austenite. Solid arrows, transformations involving diffusion; dashed arrow, diffusionless transformation.

Table 10.2 Summary of Microstructures and Mechanical Properties for Iron–Carbon Alloys

Microconstituent	*Phases Present*	*Arrangement of Phases*	*Mechanical Properties (Relative)*
Spheroidite	α Ferrite + Fe_3C	Relatively small Fe_3C sphere-like particles in an α-ferrite matrix	Soft and ductile
Coarse pearlite	α Ferrite + Fe_3C	Alternating layers of α ferrite and Fe_3C that are relatively thick	Harder and stronger than spheroidite, but not as ductile as spheroidite
Fine pearlite	α Ferrite + Fe_3C	Alternating layers of α ferrite and Fe_3C that are relatively thin	Harder and stronger than coarse pearlite, but not as ductile as coarse pearlite
Bainite	α Ferrite + Fe_3C	Very fine and elongated particles of Fe_3C in an α-ferrite matrix	Hardness and strength greater than fine pearlite; hardness less than martensite; ductility greater than martensite
Tempered martensite	α Ferrite + Fe_3C	Very small Fe_3C sphere-like particles in an α-ferrite matrix	Strong; not as hard as martensite, but much more ductile than martensite
Martensite	Body-centered tetragonal, single phase	Needle-shaped grains	Very hard and very brittle

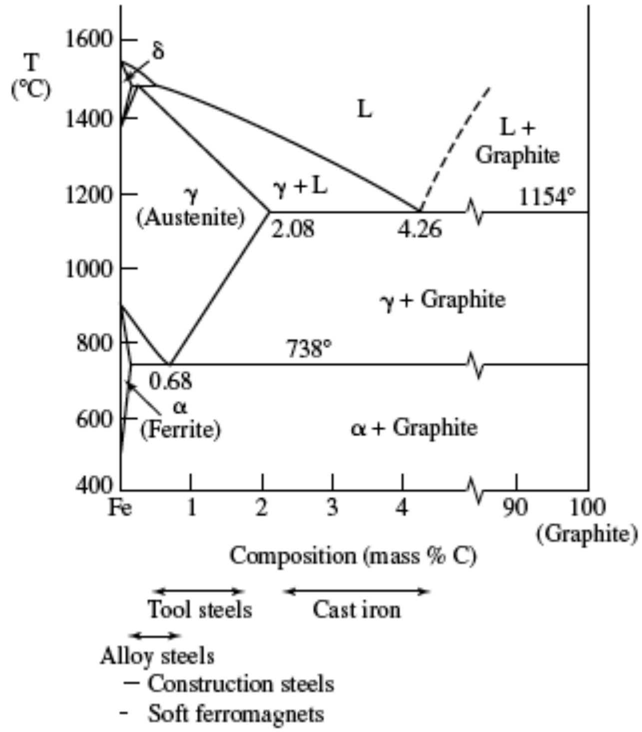

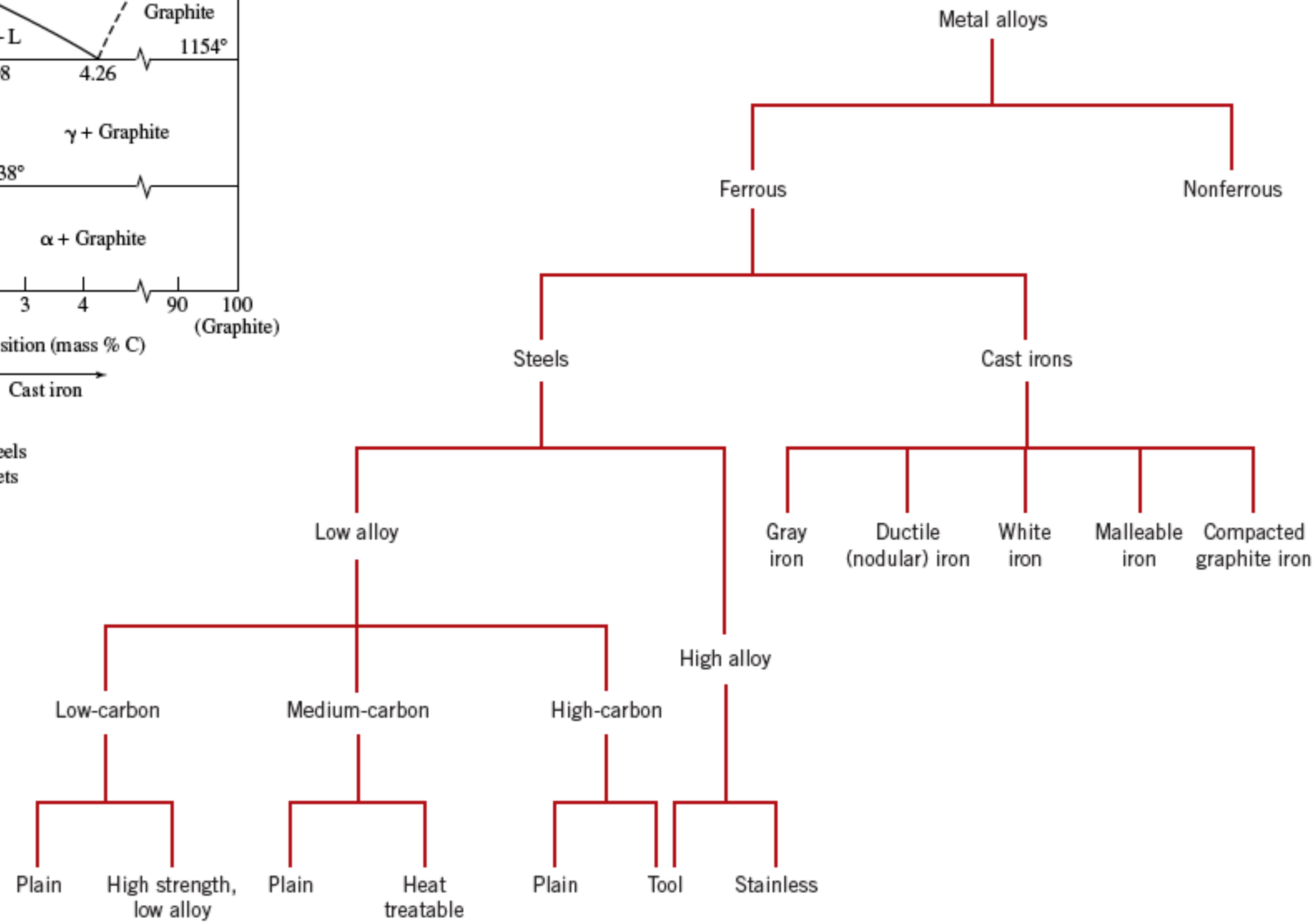

Figure 11.1 Classification scheme for the various ferrous alloys.

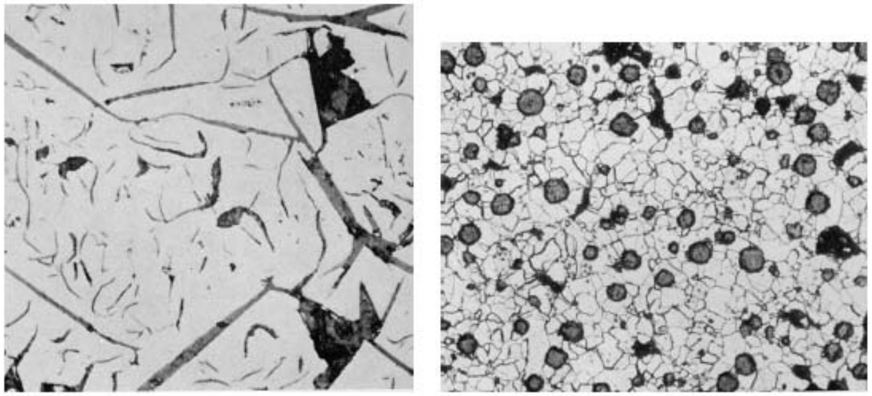

(a) (b)

FIGURE 8.8. Photomicrographs of (a) graphite flakes in gray cast iron (as polished, not etched, 100×), and (b) nodular or ductile cast iron (annealed for 6 hr at 788°C and furnace cooled, 100× 3% nitel etch). Reprinted with permission from Metals Handbook, 8th Edition, Vol. 7 (1972), ASM International, Materials Park, OH, Figures 647 and 709, respectively, pages 82 and 89, respectively.

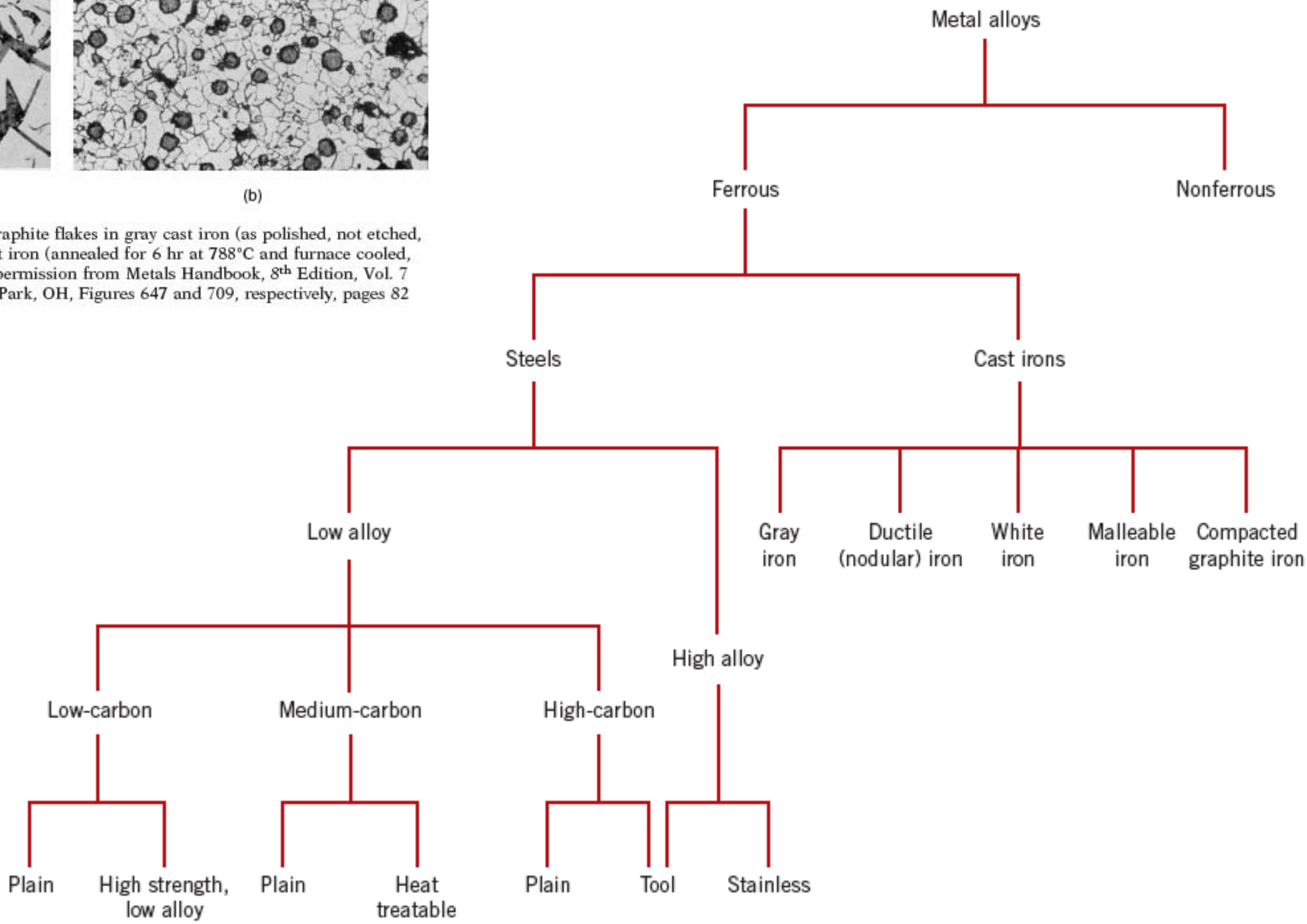

Figure 11.1 Classification scheme for the various ferrous alloys.

Table 11.1a Compositions of Five Plain Low-Carbon Steels and Three High-Strength, Low-Alloy Steels

Designation[a]		*Composition (wt%)*[b]		
AISI/SAE or ASTM Number	*UNS Number*	*C*	*Mn*	*Other*
		Plain Low-Carbon Steels		
1010	G10100	0.10	0.45	
1020	G10200	0.20	0.45	
A36	K02600	0.29	1.00	0.20 Cu (min)
A516 Grade 70	K02700	0.31	1.00	0.25 Si
		High-Strength, Low-Alloy Steels		
A440	K12810	0.28	1.35	0.30 Si (max), 0.20 Cu (min)
A633 Grade E	K12002	0.22	1.35	0.30 Si, 0.08 V, 0.02 N, 0.03 Nb
A656 Grade 1	K11804	0.18	1.60	0.60 Si, 0.1 V, 0.20 Al, 0.015 N

[a] The codes used by the American Iron and Steel Institute (AISI), the Society of Automotive Engineers (SAE), and the American Society for Testing and Materials (ASTM), and in the Uniform Numbering System (UNS) are explained in the text.

[b] Also a maximum of 0.04 wt% P, 0.05 wt% S, and 0.30 wt% Si (unless indicated otherwise).

Source: Adapted from *Metals Handbook: Properties and Selection: Irons and Steels,* Vol. 1, 9th edition, B. Bardes (Editor), American Society for Metals, 1978, pp. 185, 407.

Table 11.1b Mechanical Characteristics of Hot-Rolled Material and Typical Applications for Various Plain Low-Carbon and High-Strength, Low-Alloy Steels

AISI/SAE or ASTM Number	*Tensile Strength [MPa (ksi)]*	*Yield Strength [MPa (ksi)]*	*Ductility [%EL in 50 mm (2 in.)]*	*Typical Applications*
		Plain Low-Carbon Steels		
1010	325 (47)	180 (26)	28	Automobile panels, nails, and wire
1020	380 (55)	205 (30)	25	Pipe; structural and sheet steel
A36	400 (58)	220 (32)	23	Structural (bridges and buildings)
A516 Grade 70	485 (70)	260 (38)	21	Low-temperature pressure vessels
		High-Strength, Low-Alloy Steels		
A440	435 (63)	290 (42)	21	Structures that are bolted or riveted
A633 Grade E	520 (75)	380 (55)	23	Structures used at low ambient temperatures
A656 Grade 1	655 (95)	552 (80)	15	Truck frames and railway cars

Table 11.2a AISI/SAE and UNS Designation Systems and Composition Ranges for Plain Carbon Steel and Various Low-Alloy Steels

AISI/SAE Designation[a]	UNS Designation	Composition Ranges (wt% of Alloying Elements in Addition to C)[b]			
		Ni	*Cr*	*Mo*	*Other*
10xx, Plain carbon	G10xx0				
11xx, Free machining	G11xx0				0.08–0.33S
12xx, Free machining	G12xx0				0.10–0.35S, 0.04–0.12P
13xx	G13xx0				1.60–1.90Mn
40xx	G40xx0			0.20–0.30	
41xx	G41xx0		0.80–1.10	0.15–0.25	
43xx	G43xx0	1.65–2.00	0.40–0.90	0.20–0.30	
46xx	G46xx0	0.70–2.00		0.15–0.30	
48xx	G48xx0	3.25–3.75		0.20–0.30	
51xx	G51xx0		0.70–1.10		
61xx	G61xx0		0.50–1.10		0.10–0.15V
86xx	G86xx0	0.40–0.70	0.40–0.60	0.15–0.25	
92xx	G92xx0				1.80–2.20Si

[a] The carbon concentration, in weight percent times 100, is inserted in the place of "xx" for each specific steel.

[b] Except for 13xx alloys, manganese concentration is less than 1.00 wt%.
Except for 12xx alloys, phosphorus concentration is less than 0.35 wt%.
Except for 11xx and 12xx alloys, sulfur concentration is less than 0.04 wt%.
Except for 92xx alloys, silicon concentration varies between 0.15 and 0.35 wt%.

Table 11.2b **Typical Applications and Mechanical Property Ranges for Oil-Quenched and Tempered Plain Carbon and Alloy Steels**

AISI Number	*UNS Number*	*Tensile Strength [MPa (ksi)]*	*Yield Strength [MPa (ksi)]*	*Ductility [%EL in 50 mm (2 in.)]*	*Typical Applications*
			Plain Carbon Steels		
1040	G10400	605–780 (88–113)	430–585 (62–85)	33–19	Crankshafts, bolts
1080[a]	G10800	800–1310 (116–190)	480–980 (70–142)	24–13	Chisels, hammers
1095[a]	G10950	760–1280 (110–186)	510–830 (74–120)	26–10	Knives, hacksaw blades
			Alloy Steels		
4063	G40630	786–2380 (114–345)	710–1770 (103–257)	24–4	Springs, hand tools
4340	G43400	980–1960 (142–284)	895–1570 (130–228)	21–11	Bushings, aircraft tubing
6150	G61500	815–2170 (118–315)	745–1860 (108–270)	22–7	Shafts, pistons, gears

[a] Classified as high-carbon steels.

Table 11.3 Designations, Compositions, and Applications for Six Tool Steels

AISI Number	*UNS Number*	*Composition (wt%)*[a]						*Typical Applications*
		C	*Cr*	*Ni*	*Mo*	*W*	*V*	
M1	T11301	0.85	3.75	0.30 max	8.70	1.75	1.20	Drills, saws; lathe and planer tools
A2	T30102	1.00	5.15	0.30 max	1.15	—	0.35	Punches, embossing dies
D2	T30402	1.50	12	0.30 max	0.95	—	1.10 max	Cutlery, drawing dies
O1	T31501	0.95	0.50	0.30 max	—	0.50	0.30 max	Shear blades, cutting tools
S1	T41901	0.50	1.40	0.30 max	0.50 max	2.25	0.25	Pipe cutters, concrete drills
W1	T72301	1.10	0.15 max	0.20 max	0.10 max	0.15 max	0.10 max	Blacksmith tools, woodworking tools

[a] The balance of the composition is iron. Manganese concentrations range between 0.10 and 1.4 wt%, depending on alloy; silicon concentrations between 0.20 and 1.2 wt% depending on alloy.

Source: Adapted from *ASM Handbook,* Vol. 1, *Properties and Selection: Irons, Steels, and High-Performance Alloys,* 1990. Reprinted by permission of ASM International, Materials Park, OH.

Table 11.4 Designations, Compositions, Mechanical Properties, and Typical Applications for Austenitic, Ferritic, Martensitic, and Precipitation-Hardenable Stainless Steels

AISI Number	*UNS Number*	*Composition (wt%)*[a]	*Condition*[b]	*Mechanical Properties* — *Tensile Strength [MPa (ksi)]*	*Yield Strength [MPa (ksi)]*	*Ductility [%EL in 50 mm (2 in.)]*	*Typical Applications*
				Ferritic			
409	S40900	0.08 C, 11.0 Cr, 1.0 Mn, 0.50 Ni, 0.75 Ti	Annealed	380 (55)	205 (30)	20	Automotive exhaust components, tanks for agricultural sprays
446	S44600	0.20 C, 25 Cr, 1.5 Mn	Annealed	515 (75)	275 (40)	20	Valves (high temperature), glass molds, combustion chambers
				Austenitic			
304	S30400	0.08 C, 19 Cr, 9 Ni, 2.0 Mn	Annealed	515 (75)	205 (30)	40	Chemical and food processing equipment, cryogenic vessels
316L	S31603	0.03 C, 17 Cr, 12 Ni, 2.5 Mo, 2.0 Mn	Annealed	485 (70)	170 (25)	40	Welding construction
				Martensitic			
410	S41000	0.15 C, 12.5 Cr, 1.0 Mn	Annealed Q & T	485 (70) 825 (120)	275 (40) 620 (90)	20 12	Rifle barrels, cutlery, jet engine parts
440A	S44002	0.70 C, 17 Cr, 0.75 Mo, 1.0 Mn	Annealed Q & T	725 (105) 1790 (260)	415 (60) 1650 (240)	20 5	Cutlery, bearings, surgical tools
				Precipitation Hardenable			
17-7PH	S17700	0.09 C, 17 Cr, 7 Ni, 1.0 Al, 1.0 Mn	Precipitation hardened	1450 (210)	1310 (190)	1–6	Springs, knives, pressure vessels

[a] The balance of the composition is iron.

[b] Q & T denotes quenched and tempered.

Source: Adapted from *ASM Handbook,* Vol. 1, *Properties and Selection: Irons, Steels, and High-Performance Alloys,* 1990. Reprinted by permission of ASM International, Materials Park, OH.

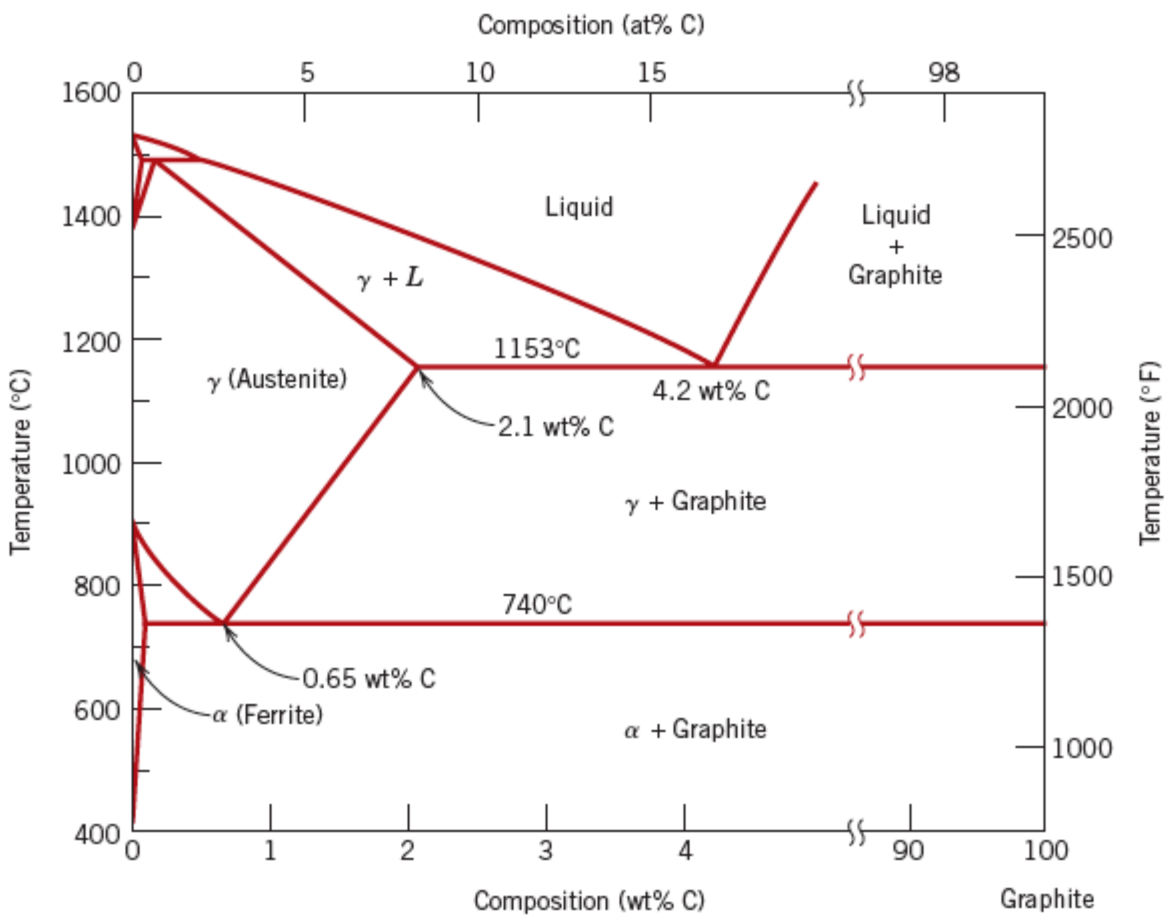

Figure 11.2 The true equilibrium iron–carbon phase diagram with graphite instead of cementite as a stable phase. [Adapted from *Binary Alloy Phase Diagrams*, T. B. Massalski, (Editor-in-Chief), 1990. Reprinted by permission of ASM International, Materials Park, OH.]

Table 11.5 Designations, Minimum Mechanical Properties, Approximate Compositions, and Typical Applications for Various Gray, Nodular, Malleable, and Compacted Graphite Cast Irons

Grade	UNS Number	Composition (wt%)[a]	Matrix Structure	Mechanical Properties: Tensile Strength [MPa (ksi)]	Mechanical Properties: Yield Strength [MPa (ksi)]	Mechanical Properties: Ductility [%EL in 50 mm (2 in.)]	Typical Applications
				Gray Iron			
SAE G1800	F10004	3.40–3.7 C, 2.55 Si, 0.7 Mn	Ferrite + Pearlite	124 (18)	—	—	Miscellaneous soft iron castings in which strength is not a primary consideration
SAE G2500	F10005	3.2–3.5 C, 2.20 Si, 0.8 Mn	Ferrite + Pearlite	173 (25)	—	—	Small cylinder blocks, cylinder heads, pistons, clutch plates, transmission cases
SAE G4000	F10008	3.0–3.3 C, 2.0 Si, 0.8 Mn	Pearlite	276 (40)	—	—	Diesel engine castings, liners, cylinders, and pistons
				Ductile (Nodular) Iron			
ASTM A536							
60–40–18	F32800	3.5–3.8 C, 2.0–2.8 Si, 0.05 Mg, <0.20 Ni, <0.10 Mo (all three grades)	Ferrite	414 (60)	276 (40)	18	Pressure-containing parts such as valve and pump bodies
100–70–03	F34800		Pearlite	689 (100)	483 (70)	3	High-strength gears and machine components
120–90–02	F36200		Tempered martensite	827 (120)	621 (90)	2	Pinions, gears, rollers, slides
				Malleable Iron			
32510	F22200	2.3–2.7 C, 1.0–1.75 Si, <0.55 Mn	Ferrite	345 (50)	224 (32)	10	General engineering service at normal and elevated temperatures (both grades)
45006	F23131	2.4–2.7 C, 1.25–1.55 Si, <0.55 Mn	Ferrite + Pearlite	448 (65)	310 (45)	6	
				Compacted Graphite Iron			
ASTM A842							
Grade 250	—	3.1–4.0 C, 1.7–3.0 Si, 0.015–0.035 Mg, 0.06–0.13 Ti (both grades)	Ferrite	250 (36)	175 (25)	3	Diesel engine blocks, exhaust manifolds, brake discs for high-speed trains (both grades)
Grade 450	—		Pearlite	450 (65)	315 (46)	1	

[a] The balance of the composition is iron.

Source: Adapted from *ASM Handbook*, Vol. 1, *Properties and Selection: Irons, Steels, and High-Performance Alloys*, 1990. Reprinted by permission of ASM International, Materials Park, OH.

Figure 11.5 From the iron–carbon phase diagram, composition ranges for commercial cast irons. Also shown are schematic microstructures that result from a variety of heat treatments. G_f, flake graphite; G_r, graphite rosettes; G_n, graphite nodules; P, pearlite; α, ferrite. (Adapted from W. G. Moffatt, G. W. Pearsall, and J. Wulff, *The Structure and Properties of Materials,* Vol. I, *Structure,* p. 195. Copyright © 1964 by John Wiley & Sons, New York. Reprinted by permission of John Wiley & Sons, Inc.)

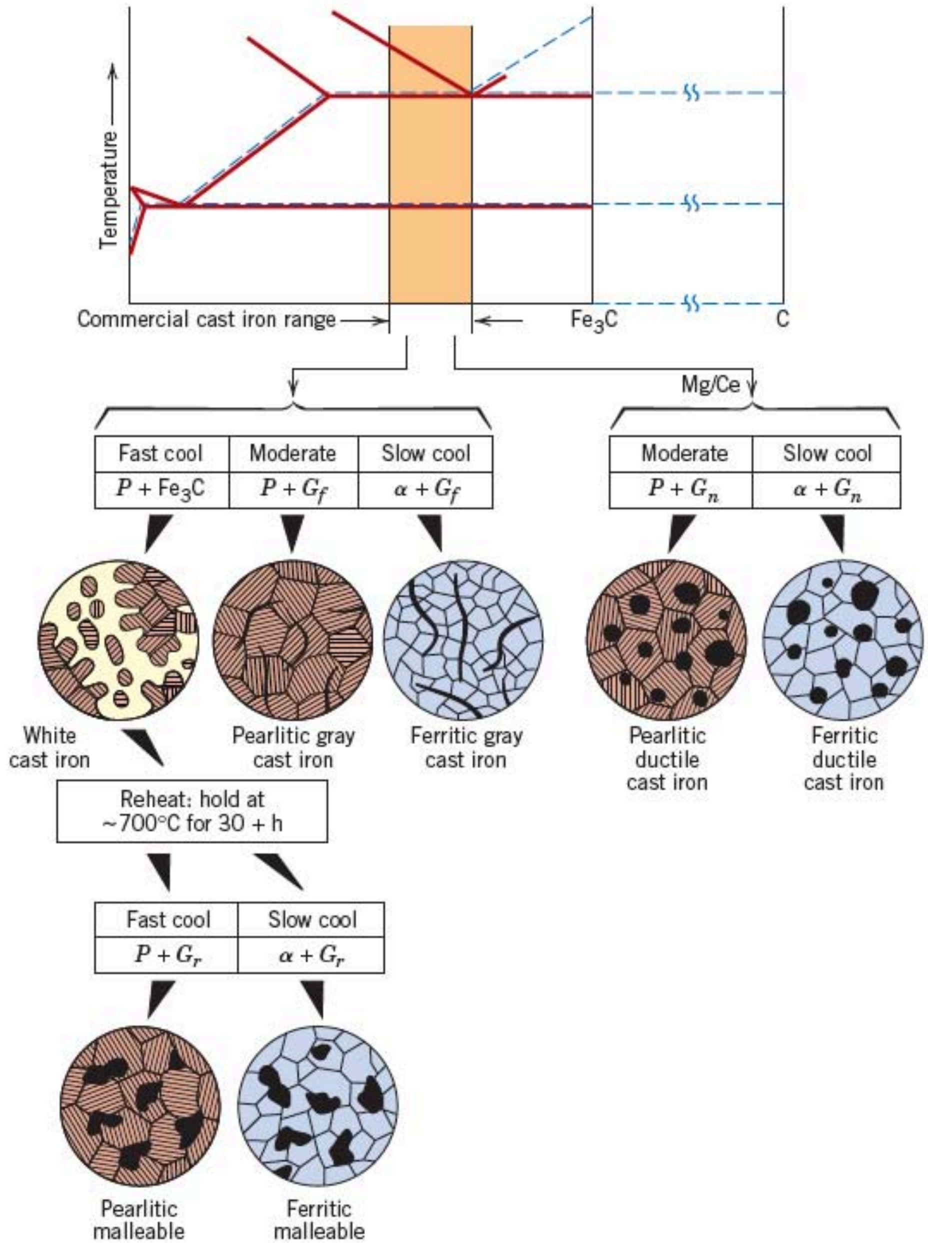

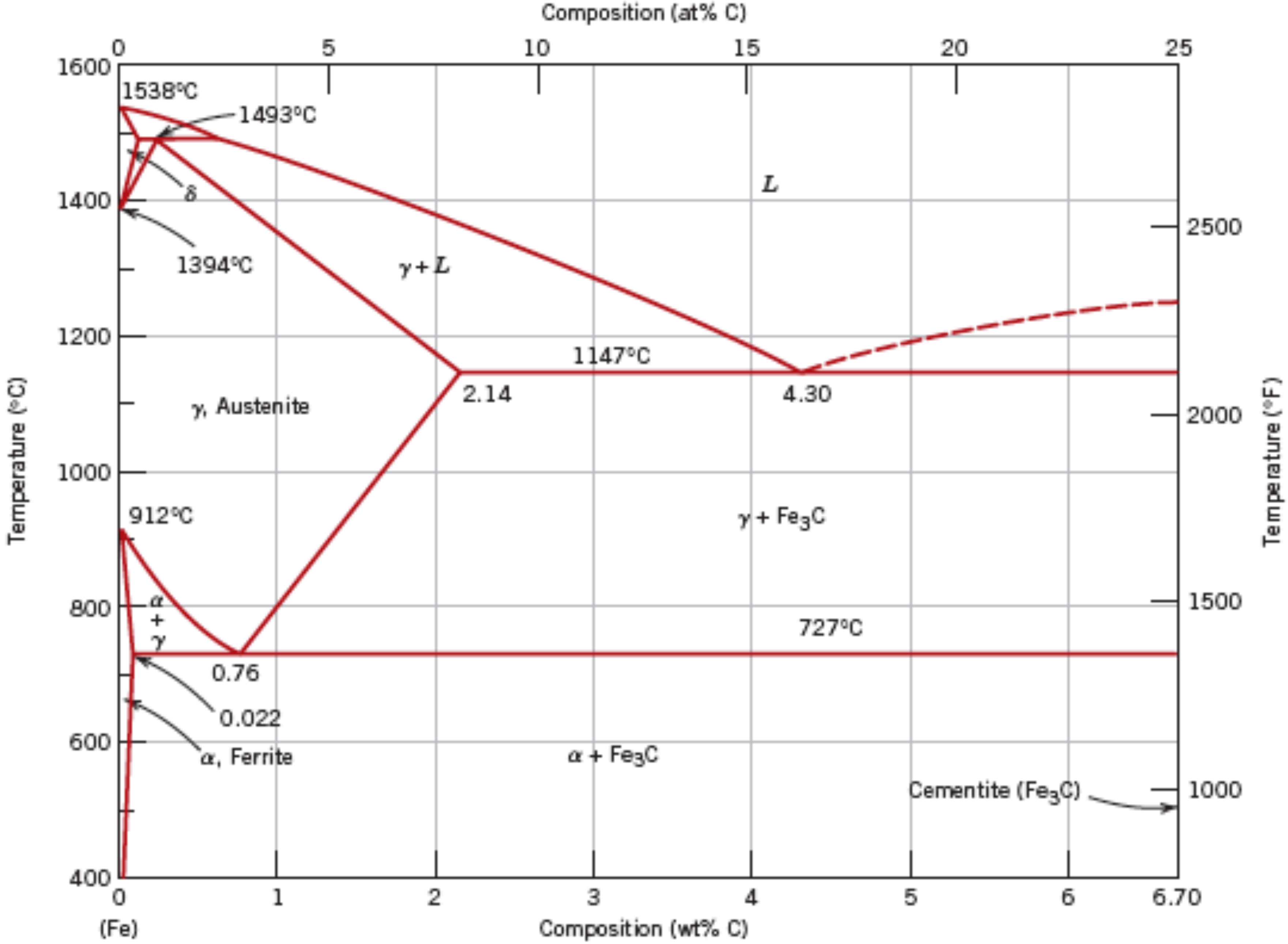

Figure 9.24 The iron–iron carbide phase diagram. [Adapted from *Binary Alloy Phase Diagrams,* 2nd edition, Vol. 1, T. B. Massalski (Editor-in-Chief), 1990. Reprinted by permission of ASM International, Materials Park, OH.]

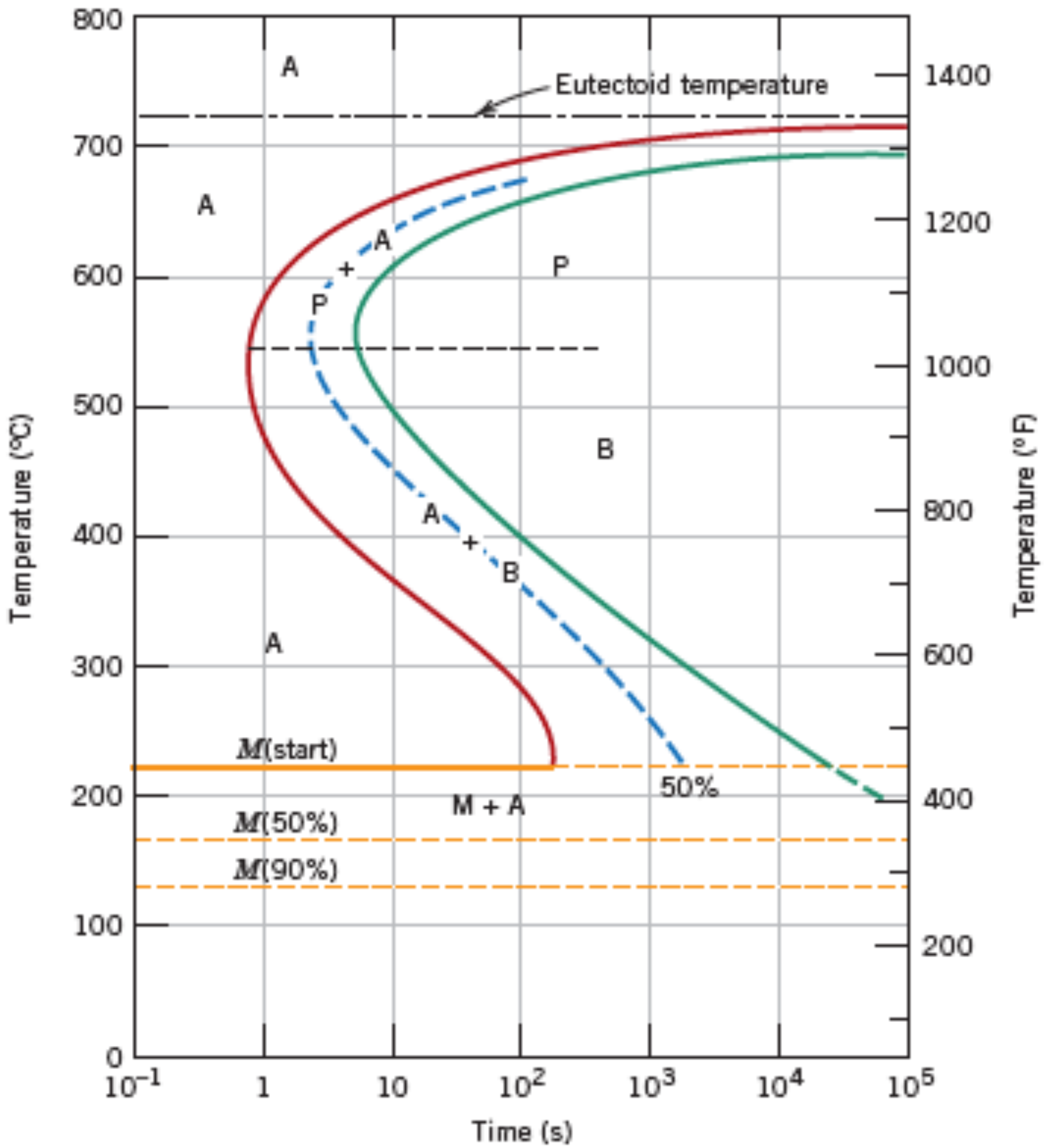

Figure 10.22 The complete isothermal transformation diagram for an iron–carbon alloy of eutectoid composition: A, austenite; B, bainite; M, martensite; P, pearlite.

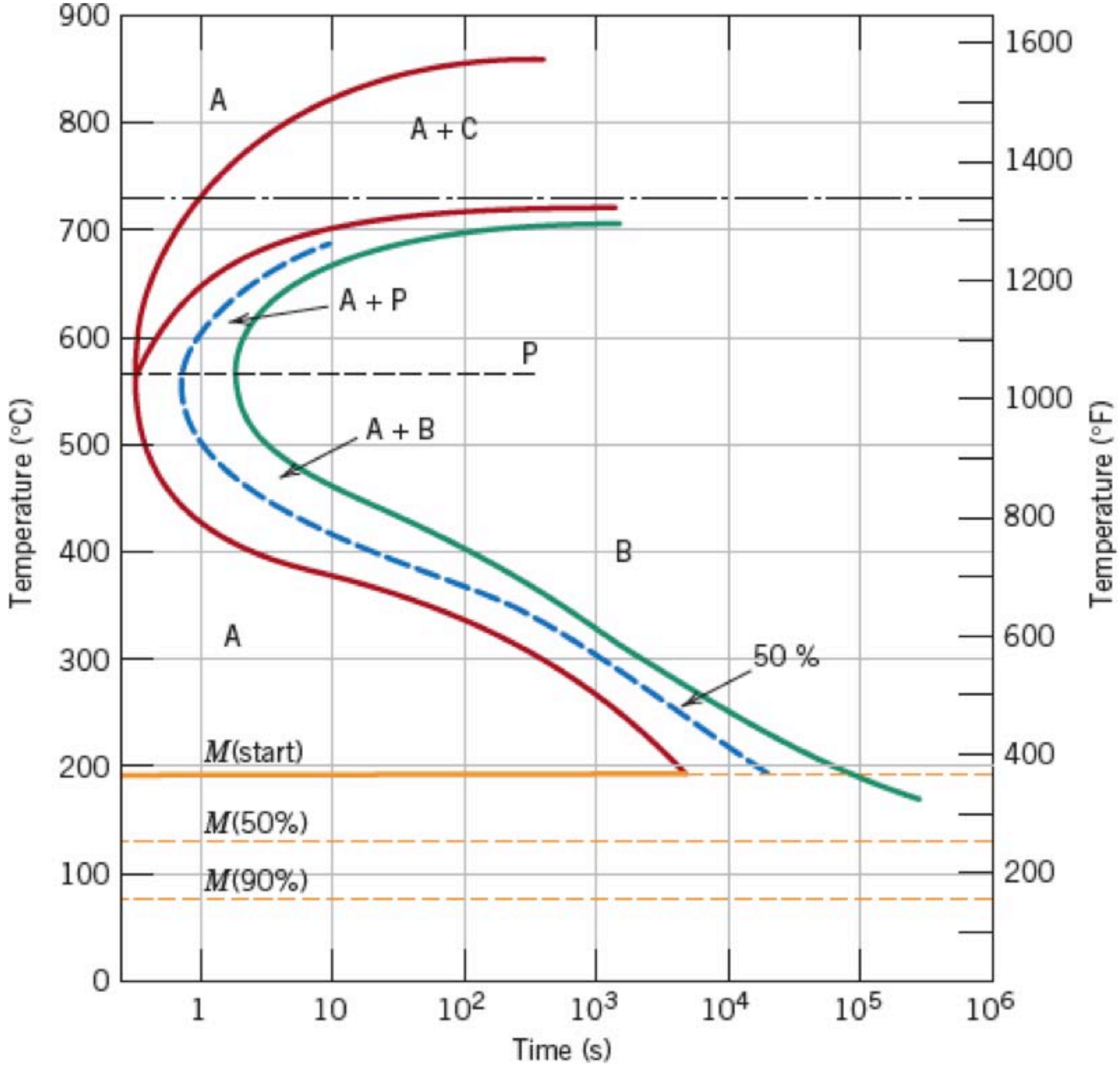

900
800
700
600
500
400
300
200
100
0
1600
1400
1200
1000
800
600
400
200
Temperature (°C)
Temperature (°F)
A
A + C
A + P
P
A + B
B
A
50 %
M(start)
M(50%)
M(90%)
1
10
10^2
10^3
10^4
10^5
10^6
Time (s)